12

APPROVED FOR PUBLIC RELEASE, DISTRIBUTION UNLIMITED

ALEX(01)-TR-76-07

ADA034925

EVALUATION OF THE IMPROVED THREE-COMPONENT ADAPTIVE PROCESSOR

TECHNICAL REPORT NO. 7

VELA NETWORK EVALUATION AND AUTOMATIC PROCESSING RESEARCH

Prepared by
Alan C. Strauss

TEXAS INSTRUMENTS INCORPORATED
Equipment Group
Post Office Box 6015
Dallas, Texas 75222

Prepared for

AIR FORCE TECHNICAL APPLICATIONS CENTER
Alexandria, Virginia 22314

Sponsored by

ADVANCED RESEARCH PROJECTS AGENCY
Nuclear Monitoring Research Office
ARPA Program Code No. 6F10
ARPA Order No. 2551

24 September 1976

Acknowledgment: This research was supported by the Advanced Research Projects Agency, Nuclear Monitoring Research Office, under Project VELA-UNIFORM, and accomplished under the technical direction of the Air Force Technical Applications Center under Contract Number F08606-76-C-0011.

APPROVED FOR PUBLIC RELEASE, DISTRIBUTION UNLIMITED

ALEX(01)-TR-76-07

EVALUATION OF THE IMPROVED THREE-COMPONENT ADAPTIVE PROCESSOR

TECHNICAL REPORT NO. 7

VELA NETWORK EVALUATION AND AUTOMATIC PROCESSING RESEARCH

Prepared by
Alan C. Strauss

TEXAS INSTRUMENTS INCORPORATED
Equipment Group
Post Office Box 6015
Dallas, Texas 75222

Prepared for

AIR FORCE TECHNICAL APPLICATIONS CENTER
Alexandria, Virginia 22314

Sponsored by

ADVANCED RESEARCH PROJECTS AGENCY
Nuclear Monitoring Research Office
ARPA Program Code No. 6F10
ARPA Order No. 2551

24 September 1976

Acknowledgment: This research was supported by the Advanced Research Projects Agency, Nuclear Monitoring Research Office, under Project VELA-UNIFORM, and accomplished under the technical direction of the Air Force Technical Applications Center under Contract Number F08606-76-C-0011.

UNCLASSIFIED

SECURITY CLASSIFICATION OF THIS PAGE (When Data Entered)

REPORT DOCUMENTATION PAGE		READ INSTRUCTIONS BEFORE COMPLETING FORM
1. REPORT NUMBER	2. GOVT ACCESSION NO.	3. RECIPIENT'S CATALOG NUMBER
4. TITLE (and Subtitle) (6) EVALUATION OF THE IMPROVED THREE-COMPONENT ADAPTIVE PROCESSOR.		5. TYPE OF REPORT & PERIOD COVERED (14) (9) Technical rept.
		6. PERFORMING ORG. REPORT NUMBER TI-ALEX(01)-TR-76-07
7. AUTHOR(s) (10) Alan C. Strauss		8. CONTRACT OR GRANT NUMBER(s) (15) F08606-76-C-0011, ARPA Order-2551
9. PERFORMING ORGANIZATION NAME AND ADDRESS Texas Instruments Incorporated Equipment Group Dallas, Texas 75222		10. PROGRAM ELEMENT, PROJECT, TASK AREA & WORK UNIT NUMBERS VELA T/6705/B/ETR
11. CONTROLLING OFFICE NAME AND ADDRESS Advanced Research Projects Agency Nuclear Monitoring Research Office Arlington, Virginia 22209		12. REPORT DATE (11) 24 September 1976
		13. NUMBER OF PAGES 77 (12) 79p.
14. MONITORING AGENCY NAME & ADDRESS (if different from Controlling Office) Air Force Technical Applications Center VELA Seismological Center Alexandria, Virginia 22314		15. SECURITY CLASS. (of this report) UNCLASSIFIED
		15a. DECLASSIFICATION/DOWNGRADING SCHEDULE

16. DISTRIBUTION STATEMENT (of this Report)

APPROVED FOR PUBLIC RELEASE, DISTRIBUTION UNLIMITED

17. DISTRIBUTION STATEMENT (of the abstract entered in Block 20, if different from Report)

18. SUPPLEMENTARY NOTES

ARPA Order No. 2551

19. KEY WORDS (Continue on reverse side if necessary and identify by block number)

Seismology	Detection Threshold	New TCA
Love Wave	Phase	
Rayleigh Wave	Azimuth	
Signal-to-Noise Ratio Gains	Original TCA	

20. ABSTRACT (Continue on reverse side if necessary and identify by block number)

Evaluation of the original three-component adaptive processor revealed that improvements in signal-to-noise ratio are much greater for Rayleigh waves than for Love waves. A new algorithm has been proposed for Love wave processing to put the effectiveness of the Love wave processor on a par with that of the Rayleigh wave processor. This new algorithm tracks the incoming Love in azimuth and passes its entire duration. In

405 076

DD FORM 1 JAN 73 1473 EDITION OF 1 NOV 65 IS OBSOLETE

UNCLASSIFIED

SECURITY CLASSIFICATION OF THIS PAGE (When Data Entered)

20. continued

addition, energy from azimuths outside some pre-set limit is rejected in a form of azimuthal filtering.

In this report, expected signal-to-noise ratio gains over the bandpass filter are determined for both the original and new versions of the three-component adaptive processor. Detection threshold improvements are then determined by applying both versions to two event suites. The evaluation is performed for both single-site and beam data.

ABSTRACT

Evaluation of the original three-component adaptive processor revealed that improvements in signal-to-noise ratio are much greater for Rayleigh waves than for Love waves. A new algorithm has been proposed for Love wave processing to put the effectiveness of the Love wave processor on a par with that of the Rayleigh wave processor. This new algorithm tracks the incoming Love in azimuth and passes its entire duration. In addition, energy from azimuths outside some pre-set limit is rejected in a form of azimuthal filtering.

In this report, expected signal-to-noise ratio gains over the bandpass filter are determined for both the original and new versions of the three-component adaptive processor. Detection threshold improvements are then determined by applying both versions to two event suites. The evaluation is performed for both single-site and beam data.

ACKNOWLEDGMENTS

We wish to thank S. Lane for many helpful discussions and criticisms made during the course of this evaluation. We also wish to thank S. Lane and L. Turnbull for their critical reading of this paper.

TABLE OF CONTENTS

LIST OF FIGURES

LIST OF FIGURES
(continued)

LIST OF TABLES

SECTION 1
INTRODUCTION

The three-component adaptive processor (TCA) was developed at the Lamont Geophysical Observatory (Shimshoni and Smith, 1964) and was evaluated for single-site and beam data by Texas Instruments, Inc. (Lane, 1973). This processor, designed to improve the detectability of long-period Rayleigh and Love waves, takes advantage of the known phase relationships among the three mutually perpendicular long-period seismometer traces. Improvements in the signal-to-noise ratio (SNR) can be achieved when these phase relationships are utilized in the processor design.

The evaluation of the original TCA processor (Lane, 1973) revealed that improvements in signal-to-noise ratio are much greater for Rayleigh wave processing than for Love wave processing. This is due to two factors. First, Love wave energy may arrive as much as 20° off the great circle azimuth, and the TCA processor suppresses this motion as though it were noise. Second, the TCA processor confuses the radial motion of the Rayleigh wave with off-azimuth Love waves, and suppresses whatever genuine Love wave energy which is present. Thus, the TCA processor has shown itself to be less effective in separating Love waves than Rayleigh waves from noise.

This report describes an attempt to rectify this situation. The TCA processor is modified to track the incoming Love wave in azimuth and to pass its entire duration. This is accomplished by using in the design of the transverse component filter the additional information contained in the phase relationships of the Rayleigh waves.

The evaluation of this modification of the TCA processor uses both synthetic and real data. The synthetic data consists of known signals with high signal-to-noise ratios buried in seismic noise. These are used to study the signal-to-noise ratio improvement characteristics of the processor. Part of the real data used consists of hour-long noise samples, which are used to determine signal detection criteria and false-alarm characteristics of the processor. The remainder of the real data consists of single-site and beam data recorded at the Alaskan Long Period Array (ALPA). This data is used to study the detection performance of the processor.

To allow direct comparisons between the original and new Love wave processors, the original Love wave processor was re-evaluated using the same data base as was used for the evaluation of the new Love wave processor. The Rayleigh wave processor was also re-evaluated, since the necessary data processing for this was performed automatically with the Love wave data processing. Use of the larger data base should improve previous estimates of Rayleigh wave detection capability improvement due to application of the TCA processor.

Section II of this report describes the theory of the TCA processor, with emphasis on the new Love wave processor. The experimental data base is also described in this section. Section III describes the single-site and beam processor gains to be expected from the TCA processor. Section IV gives the results of evaluating the detection capability improvement due to the TCA processor. Conclusions regarding the method are presented in Section V.

SECTION II

METHOD OF EVALUATION

A. DESCRIPTION OF THE THREE-COMPONENT ADAPTIVE PROCESSOR

The three-component adaptive processor forms Love and Rayleigh wave filters in the frequency domain, which pass energy having the phase characteristics of these waveforms. The filters are adaptive, since the data are segmented and new filters are designed for each segment. The filter weights depend only on the signal behavior during the segment.

The Rayleigh wave filter algorithm will not be discussed in detail here, since it is throughly described in earlier reports (Lane, 1973; Strauss and Tolstoy, 1974). In general, the method is as follows. To pass Rayleigh waves, the processor seeks signals which are 90° out of phase on the vertical and radial components. The Fourier transform of a segment of data is taken. The phase angle θ between the radial and vertical components is then calculated at each frequency. This angle will be $\pi/2$ for pure Rayleigh motion. The filter weight at each frequency is calculated from:

$$F(i) = \sin^N \left(\theta (i) \right) .$$

(In this evaluation, we used N=8.) The Fourier components at each frequency are then multiplied by the corresponding filter weight. Finally, the data are inverse transformed. Processing is performed on 64-point segments with fifty percent segment overlap.

The computation method of the original Love wave portion of the TCA processor rests on the fact that, when the components are properly

oriented, the Love wave appears only on the transverse component. The Love wave filter weights are as follows:

$$G(i) = \cos^N\left(\gamma(i)\right)$$

where γ is the angle between the transverse component and the actual Love wave particle motion. The exponent N is the same as for the Rayleigh wave filter. This filter will pass in full only that energy which has the characteristics of on-azimuth Love waves.

The new method of handling the Love wave is to track the incoming energy in azimuth and to pass it throughout its entire duration. This is performed in the following manner for each frequency component. First, the time origin is shifted so that the vertical component is purely real. Next, the propagation direction β (Figure II-1) of the transverse component energy relative to the radial direction is calculated. Following this, the horizontal components are rotated about the vertical axis by $-\beta$ with the result that all Love wave motion lies on the transverse component. After each frequency component has been rotated in this fashion, the time origin is shifted back. Finally, the Fourier transformation with fifty percent overlapping of adjacent segments, as in the original TCA processor, will yield the complete Love wave time history. The equations relevant to this process are given in the following paragraphs.

After shifting the time origin so that the vertical component is purely real (has zero phase), we have:

$$Z_r = P \tag{II-1}$$

$$Z_i = O \tag{II-2}$$

$$R_r = L \cos \psi \sin \beta \tag{II-3}$$

$$R_i = L \sin \psi \sin \beta + P\cos \alpha P \cos \epsilon \tag{II-4}$$

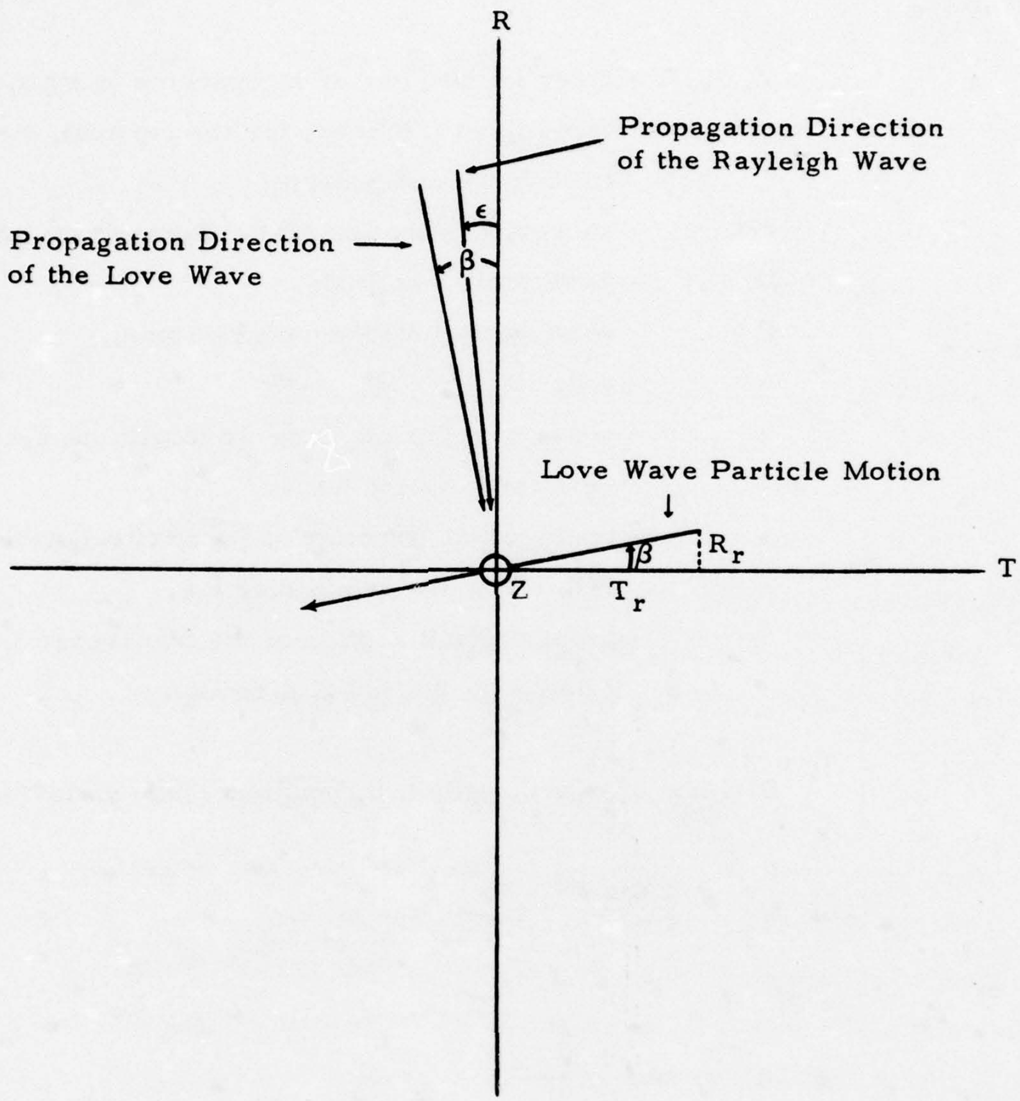

FIGURE II-1

LOVE AND RAYLEIGH ARRIVAL AZIMUTHS FOR AN ARBITRARY FREQUENCY COMPONENT

$$T_r = L \cos \psi \cos \beta \qquad \text{(II-5)}$$

$$T_i = L \sin \psi \cos \beta + \alpha P \sin \epsilon \alpha P \sin \epsilon \qquad \text{(II-6)}$$

where

Z, R, T - refer to the Fourier components of motion at the same fixed frequency for the vertical, radial, and transverse components,

r, i - subscripts denoting real and imaginary parts,

L - Love wave amplitude,

P - vertical Rayleigh wave amplitude,

α - ellipticity,

ψ - phase angle of the Love wave with respect to the vertical Rayleigh wave,

ϵ - propagation direction of the vertical Rayleigh wave relative to the radial diretion,

β - propagation direction of the transverse Love wave relative to the radial direction.

Division of equation (II-3) by equation (II-5) yields the angle β:

$$\frac{R_r}{T_r} = \frac{L \cos \psi \sin \beta}{L \cos \psi \cos \beta} = \tan \beta \qquad \text{(II-7)}$$

or

$$\beta = \tan^{-1} \frac{R_r}{T_r} \quad . \qquad \text{(II-8)}$$

Rotation of the horizontal components by the angle $-\beta$ about the vertical axis yields:

$$Z_r = P \tag{II-9}$$

$$Z_i = O \tag{II-10}$$

$$R_r' = O \tag{II-11}$$

$$R_i' = \alpha P \cos(\epsilon - \beta) \tag{II-12}$$

$$T_r' = L \cos \psi \tag{II-13}$$

$$T_i' = L \sin \psi + \alpha \; P \sin(\epsilon - \beta) . \tag{II-14}$$

Under the reasonable assumption that ϵ and β are about the same, equations (II-12) and (II-14) become, respectively,

$$R_i' = \alpha P \tag{II-15}$$

$$T_i' = L \sin \psi . \tag{II-16}$$

After each frequency component has been rotated in this way, the origin is time shifted back and an inverse Fourier transformation with fifty percent overlapping of adjacent segments as in the original TCA processor will yield the complete Love wave time history. A listing and description of usage of the new TCA processor program are given in Appendix A.

Before proceeding to the evaluation of the new Love wave TCA processor, two points must be discussed. The first point to be considered is the case where the phase angle ψ of the Love wave relative to the vertical Rayleigh wave is $\pi/2$. Reference to equations (II-3) and (II-5) of this section shows that, in this case, the angle β cannot be determined, since both T_r and R_r will be zero; therefore no rotation will take place. Although the TCA processed trace will not be degraded relative to the unprocessed trace in this case, we cannot expect much signal-to-noise ratio improvement if this is a frequent occurrence.

We cannot easily compute ψ directly, but we can check T_r and R_r. Assuming L is not zero, if both T_r and R_r are zero simultaneously, ψ must be $\pi/2$. Therefore, the values of T_r and R_r as calculated by the new TCA processor were printed out for several events. Examination of these values did not reveal any occurrences of this situation. Thus, this matter should pose no problem in the operation of the new TCA processor.

The second point to be considered is that a high signal-to-noise ratio on the vertical axis is required to accurately pick the time origin so that the vertical Rayleigh wave Fourier component is purely real. The Rayleigh wave filter calculates a measure of this signal-to-noise ratio in the phase angle between the radial and vertical motion. It was originally proposed that when this is near 90°, little noise would be present; therefore, the time shift could be performed accurately, while in other cases no time shifts would occur. However, further consideration of this matter shows that for small signals (at or near the noise level) the signal-to-noise ratio is so low that no processing would occur. Since it is precisely these signals which we most want to enhance, no restriction of the type described above was used in this evaluation.

B. DATA BASE

Suites of events from the southern Kamchatka and central Asia seismic regions were selected for this evaluation of the new TCA processor. Two regions were chosen rather than one to allow a judgment to be made as to whether the effects of the TCA processor vary greatly from region to region. These regions were defined in the final report on ALPA (Strauss, 1973).

The only restrictions placed on event selection were that the data were required to be free of spikes and long-period transients and unmixed with other signals and that the single site and beam traces be 4096 seconds in

length. There were a total of 86 events available from the southern Kamchatka (SKAM) region and 76 events from the central Asia (CENA) region. The parameters of these events are listed in Tables II-1 and II-2, respectively. We note that the event numbers listed under the column headed 'EVNO' are as used by Lambert in his evaluation of the Very Long Period Experiment stations (Lambert, et al., 1974). The column headed 'EVENT NAME' lists the unique twelve-character name assigned to each seismic event. The columns headed 'DATE' and 'ORIGIN TIME' give the date and time of occurrence of each event. The epicentral coordinates are listed in the columns headed 'LATITUDE' and 'LONGITUDE'. The column headed 'DEP' gives, when known, the depth to the hypocenter of the event. The column headed 'MB' gives the bodywave magnitude of each event. The last column, headed 'IS', gives the information source for the listed event parameters, where P stands for the PDE (Preliminary Determination of Epicenters) event lists, L stands for the LASA (Large Aperature Seismic Array) event lists, N stands for the NORSAR (Norwegian Seismic Array) event lists, and I and J stand for the verified and unverified International Seismic Month event lists, respectively.

TABLE II-1

SOUTHERN KAMCHATKA EVENTS
(PAGE 1 OF 2)

EVNO	EVENT NAME	DATE	ORIGIN TIME	EPICENTER LAT.	EPICENTER LONG.	DEP	MB	TS
B004	KAM*163*07AL	6/12/71	7.25. 0	52.0 N	159.0 E	--	3.5	L
B010	KUR*181*09AL	6/30/71	9.31.20	50.0 N	158.0 E	--	3.8	L
B021	KUR*199*12OC	7/18/71	12.32.38	51.0 N	157.0 E	--	4.3	L
B024	KAM*204*08AL	7/23/71	8. 1.23	52.7 N	160.7 E	33	4.8	P
B030	KAM*205*08AL	7/25/71	8.12.34	53.0 N	160.0 E	--	3.7	L
B032	KUR*213*02AL	8/ 1/71	2. 6. 7	50.4 N	156.8 E	20	5.6	P
B034	KAM*217*01AL	8/ 5/71	1. 5.57	50.0 N	156.8 E	--	3.7	L
B039	KAM*225*00AL	8/13/71	0.34.44	49.0 N	156.0 E	--	3.7	L
C003	KUR-001-18AL	1/ 1/72	18.13.54	49.4 N	156.5 E	--	4.0	L
C007	KAM-003-06AL	1/ 3/72	6.36.38	51.6 N	159.4 E	N	4.8	P
C028	KOM-009-03OI	1/ 9/72	3.23. 6	54.4 N	164.4 E	--	3.6	L
C033	KOM-011-08AL	1/11/72	8.54.34	54.7 N	168.2 E	--	3.9	L
C042	KUR-015-00AL	1/15/72	0.58.33	49.6 N	155.0 E	--	3.9	L
C058	KAM-024-12AL	1/24/72	12.39.29	51.7 N	158.0 E	--	4.0	L
C059	KAM-025-10AL	1/25/72	10. 2.40	53.9 N	160.9 E	N	4.6	P
C069	KUR-026-15AL	1/26/72	15.56.27	48.9 N	155.9 E	--	4.8	L
C086	KUR-033-17AL	2/ 2/72	17.56.39	50.7 N	160.1 E	--	3.6	L
C139	KAM-052-22AL	2/21/72	22. 0.59	54.4 N	161.3 E	N	4.8	I
C220	KAM-061-16AL	3/ 1/72	16.58.59	51.0 N	162.0 E	N	3.5	J
C222	KOM-062-06OC	3/ 2/72	6.17.29	53.0 N	167.0 E	N	3.6	I
C227	KAM-063-00AL	3/ 3/72	0.39.23	53.0 N	159.2 E	N	4.1	I
C233	KUR-063-23AL	3/ 3/72	23.10.41	50.2 N	155.7 E	N	4.5	I
C271	KUR-073-02AL	3/13/72	2.11. 5	49.0 N	158.0 E	N	3.8	I
C292	KUR-077-07AL	3/17/72	7.49. 2	49.0 N	156.2 E	33	5.2	I
C386	KOM-171-01AL	6/19/72	1.43.48	54.4 N	168.6 E	33	5.0	P
C389	KUR-171-22AL	6/19/72	22.41.42	48.0 N	157.0 E	--	4.1	L
C396	KAM-173-10OC	6/21/72	10.42.45	54.0 N	161.0 E	--	4.3	L
C411	KAM-177-17AL	6/25/72	17.35.50	54.0 N	160.0 E	--	4.1	L
C417	KAM-179-06AL	6/27/72	6.49. 3	54.0 N	159.0 E	--	3.8	L
C428	KAM-180-14AL	6/28/72	14.58.49	53.0 N	161.0 E	--	3.9	L
C505	KAM-199-08AR	7/17/72	8.28.52	55.0 N	159.6 E	33	5.3	P
C581	KUR-218-22AL	8/ 5/72	22.11.52	49.0 N	155.0 E	--	3.8	L
C653	KAM-233-08OC	8/20/72	8.10. 8	51.3 N	161.6 E	N	5.2	P
C664	KUR-236-10AL	8/23/72	10.38. 8	49.0 N	156.0 E	--	3.7	L
C668	KAM-237-17AL	8/24/72	17. 5.56	53.0 N	160.0 E	--	3.8	L
C681	KUR-241-09AL	8/28/72	9. 0.22	49.0 N	155.0 E	--	3.7	L
C691	KAM-243-20AL	8/30/72	20. 6.50	53.0 N	160.0 E	--	4.6	L
C737	KAM-323-08AL	11/18/72	8.31.16	52.7 N	160.2 E	N	4.6	P
C764	KAM-332-21TD	11/27/72	21.37.47	53.4 N	161.3 E	45	4.7	P
C776	KAM-336-21AL	12/ 1/72	21.15.52	54.9 N	162.0 E	33	4.8	P
C783	KAM-338-13AL	12/ 3/72	13.13.13	53.8 N	160.6 E	33	4.4	P
C815	KAM-347-00AL	12/12/72	0.36. 4	53.1 N	160.0 E	40	4.7	P
C843	KUR-353-20AL	12/18/72	20.48.20	49.0 N	160.0 E	--	3.8	L

TABLE II-1

SOUTHERN KAMCHATKA EVENTS
(PAGE 2 OF 2)

EVNO	EVENT NAME	DATE	ORIGIN TIME	EPICENTER LAT.	EPICENTER LONG.	DEP	MB	IS
0846	KUR-355-11AL	12/20/72	11. 9. 2	50.0 N	159.0 E	--	4.1	L
0852	KUR-357-07AL	12/22/72	7.33. 7	49.0 N	156.0 E	--	4.1	L
0859	KAM-360-18AL	12/25/72	18.55.58	53.0 N	159.4 E	52	5.7	P
0869	KOM-364-11TD	12/29/72	11.26.29	53.8 N	169.0 E	17	4.3	P
0882	KUR+003+06AL	1/ 3/73	6.17.10	51.0 N	157.0 E	--	4.1	L
0888	KUR+004+13AL	1/ 4/73	13.35.56	51.0 N	158.0 E	--	3.5	L
0893	KUR+006+15AL	1/ 6/73	15. 5.38	49.3 N	155.5 E	34	4.7	P
0894	KAM+008+23AL	1/ 8/73	23.[illegible]7.30	52.0 N	159.0 E	--	3.9	L
0901	KAM+012+08AL	1/12/73	8.15. 5	53.0 N	163.0 E	--	3.8	L
0904	KAM+012+22AL	1/12/73	22.10.48	54.0 N	161.0 E	--	3.9	L
0959	NKA+051+20AL	2/20/73	20. 2.39	53.6 N	169.6 E	33	4.6	P
0976	KAM+057+18AL	2/26/73	18. 0.17	51.0 N	160.0 E	--	3.8	L
0981	KAM+058+04AL	2/27/73	4.58. 9	54.0 N	170.0 E	--	4.0	L
1006	KAM+059+20AL	2/28/73	20.16.19	50.0 N	158.0 E	--	3.9	L
1008	SKA+060+02RR	3/ 1/73	2.19. 3	49.8 N	157.2 E	30	5.5	P
1013	SKA+060+09RR	3/ 1/73	9.33.16	51.0 N	158.0 E	--	4.4	L
1024	SKA+061+10AL	3/ 2/73	10.24.45	50.0 N	158.0 E	--	4.1	L
1025	SKA+061+11AL	3/ 2/73	11.11.37	51.0 N	158.0 E	--	4.2	L
1029	SKA+062+02AL	3/ 3/73	2.42. 9	50.4 N	156.2 E	59	5.5	P
1032	SKA+062+09AL	3/ 3/73	9.12.11	51.0 N	158.0 E	--	4.6	L
1040	SKA+063+22AL	3/ 4/73	22.53. 7	48.0 N	155.0 E	--	4.2	L
1041	SKA+064+06AL	3/ 5/73	6.15.54	51.0 N	158.0 E	--	4.0	L
1043	SKM+064+19AL	3/ 5/73	19.48.58	51.0 N	158.0 E	--	3.9	N
1046	SKA+065+02AL	3/ 6/73	2.19. 8	50.0 N	158.0 E	--	3.6	L
1061	SKA+067+20RR	3/ 8/73	20.12.27	51.0 N	158.0 E	--	4.5	L
1071	SKA+069+04RR	3/10/73	4.44.41	50.7 N	156.7 E	33	4.7	P
1083	SKA+071+11AL	3/12/73	11.14.23	50.1 N	156.7 E	49	5.7	P
1085	SKA+071+19AL	3/12/73	19.39.21	50.8 N	157.1 E	54	6.1	P
1104	SKA+079+14AL	3/20/73	14.27.57	49.0 N	155.0 E	--	4.5	N
1114	SKA+081+10RR	3/22/73	10.41. 2	53.0 N	160.0 E	--	4.2	L
1120	SKA+082+03AL	3/23/73	3.59.13	51.0 N	157.0 E	--	4.4	L
1121	SKA+083+02AL	3/24/73	2.50.57	51.0 N	158.0 E	--	4.5	L
1123	SKA+083+07AL	3/24/73	7.14.26	51.6 N	161.6 E	33	4.8	P
1125	SKA+084+08AL	3/25/73	8.56.15	50.2 N	156.9 E	40	5.4	P
1140	SKA+086+16AL	3/27/73	16.56.30	51.0 N	158.0 E	--	4.1	L
1151	SKA+090+20AL	3/31/73	20.45.31	50.2 N	157.1 E	44	4.8	P
1212	SKA+098+06AL	4/ 8/73	6.39.25	52.1 N	158.6 E	33	4.3	P
1226	NKA+104+13AL	4/14/73	13.46.11	53.0 N	163.0 E	--	3.7	L
1229	SKA+105+03AL	4/15/73	3.13.11	51.0 N	158.0 E	--	4.1	L
1247	NKA+113+18AL	4/23/73	18.31.46	54.0 N	163.0 E	--	4.0	L
1248	SKA+114+03AL	4/24/73	3.35.36	51.0 N	158.0 E	--	3.9	L
1250	SKA+114+20AL	4/24/73	20.15.37	49.0 N	155.0 E	--	4.1	L
1265	SKA+120+14AL	4/30/73	14.45.33	54.0 N	160.0 E	--	3.7	L

TABLE II-2

CENTRAL ASIA EVENTS
(PAGE 1 OF 2)

EVNO	EVENT NAME	DATE	ORIGIN TIME	EPICENTER LAT.	EPICENTER LONG.	DEP	MB	IS
B044	SIN*237*060C	8/25/71	6.15.23	40.5 N	77.2 E	15	4.4	L
B049	KAZ*273*12AL	9/30/71	12.43.45	50.0 N	88.0 E	--	4.5	N
B053	SIN*281*09AL	10/ 8/71	9.20.15	41.0 N	79.0 E	--	4.4	L
B062	TIB*302*17AL	10/29/71	17.16.52	34.0 N	86.0 E	--	5.0	N
0107	TIB-037-04AL	2/ 6/72	4.29. 5	29.0 N	89.0 E	--	4.1	N
0108	SIN-037-07AL	2/ 6/72	7.30.11	41.6 N	82.2 E	33	4.7	P
0120	SIN-042-05OD	2/11/72	5.55.46	39.9 N	77.4 E	23	4.9	P
0121	TIB-042-12AL	2/11/72	12.20.43	29.0 N	87.0 E	--	4.3	N
0144	HIN-053-08OC	2/22/72	8.14.26	36.6 N	68.6 E	N	4.0	J
0172	USM-057-23AL	2/26/72	23.31.10	50.6 N	97.3 E	N	5.3	I
0183	AUB-059-05OX	2/28/72	5.18.56	36.7 N	71.4 E	N	4.2	I
0186	CRS-059-15OX	2/28/72	15.44.20	51.8 N	90.2 E	N	3.9	I
0217	BTN-061-05AL	3/ 1/72	5. 6.22	27.0 N	89.0 E	N	3.9	J
0236	SIN-064-08AL	3/ 4/72	8.22.16	42.1 N	83.3 E	N	4.4	I
0275	TIB-073-18AL	3/13/72	18.27. 7	34.0 N	93.0 E	N	4.1	J
0319	KZS-154-05AL	6/ 2/72	5.11.13	43.0 N	81.0 E	--	3.5	N
0320	SIN-154-06AL	6/ 2/72	6.30.49	42.0 N	81.0 E	--	3.9	N
0322	CIN-154-20AL	6/ 2/72	20.32.55	28.4 N	95.9 E	33	4.3	P
0382	TIB-170-04AL	6/18/72	4.30.47	33.0 N	93.0 E	--	4.3	N
0384	TSK-170-09OC	6/18/72	9.18.49	40.0 N	73.0 E	--	4.3	L
0392	KIB-172-15AL	6/20/72	15.34.37	32.0 N	75.0 E	--	3.6	N
0403	TSK-175-16AL	6/23/72	16.59.48	37.0 N	75.0 E	--	3.7	N
0410	HIN-177-07AL	6/25/72	7.55.45	36.3 N	69.6 E	46	4.7	P
0414	HIN-178-20AL	6/26/72	20.59. 3	36.0 N	69.0 E	--	3.7	N
0418	BUR-179-09AL	6/27/72	9. 5.53	26.2 N	96.6 E	23	4.4	P
0421	HIN-179-15AL	6/27/72	15.59.35	36.3 N	69.5 E	53	5.1	P
0423	TSI-180-03AL	6/28/72	3. 9.59	33.0 N	91.0 E	--	3.6	N
0449	SIN-187-01AL	7/ 5/72	1. 9.53	44.6 N	81.1 E	N	4.6	P
0451	SIN-187-04AL	7/ 5/72	4. 9.49	43.6 N	87.9 E	N	4.3	P
0656	SIK-234-14AL	8/21/72	14. 4.34	27.2 N	88.0 E	N	4.8	P
0677	HIN-240-16AL	8/27/72	16.54. 1	36.0 N	70.0 E	--	3.6	N
0685	TIB-242-23AL	8/29/72	23. 0.21	34.0 N	82.0 E	--	3.7	N
0687	TSI-243-15AL	8/30/72	15.14.10	36.7 N	96.5 E	N	5.5	P
0688	SIN-243-17AL	8/30/72	17.52.23	40.0 N	94.0 E	--	4.2	N
0693	CRS-244-14AL	8/31/72	14. 3.16	52.3 N	95.4 E	N	5.5	P
0708	SIK-311-10RR	11/ 6/72	10.56. 9	27.0 N	88.7 E	N	4.8	P
0722	KSB-316-14TE	11/11/72	14. 8.58	41.0 N	77.0 E	--	3.8	N
0729	AUB-320-14OC	11/15/72	14.56.53	37.0 N	73.0 E	--	3.9	N

TABLE II-2

CENTRAL ASIA EVENTS
(PAGE 2 OF 2)

EVNO	EVENT NAME	DATE	ORIGIN TIME	EPICENTER LAT.	EPICENTER LONG.	DEP	MB	IS
0732	BUR-321-11RR	11/16/72	11.24.12	24.0 N	96.0 E	--	4.4	N
0743	SIN-325-05QR	11/20/72	5.37.12	43.0 N	84.0 E	--	4.0	N
0781	SIN-338-08AL	12/ 3/72	8.54.47	39.4 N	75.3 E	33	5.0	P
0788	PAK-339-22AL	12/ 4/72	22.58.21	35.0 N	72.0 E	--	3.9	N
0845	AFG-355-04AL	12/20/72	4.15.29	31.0 N	67.0 E	--	4.3	N
0847	PAK-355-13AL	12/20/72	13. 9.46	32.0 N	72.0 E	--	3.7	N
0854	SIN-357-23AL	12/22/72	23.20.33	36.0 N	85.0 E	--	3.8	N
0855	PAK-359-19AL	12/24/72	19.11.28	35.0 N	72.0 E	--	4.0	N
0870	TIB-365-05TD	12/30/72	5.25.49	30.0 N	85.0 E	--	4.1	N
0873	TIB-365-13AL	12/30/72	13.29.36	33.7 N	87.6 E	33	4.5	P
0884	TAD+003+14AL	1/ 3/73	14.31. 4	39.1 N	71.9 E	33	5.5	P
0886	PAK+003+17AL	1/ 3/73	17. 4.43	34.0 N	72.0 E	--	3.8	N
0896	AFG+010+03AL	1/10/73	3. 2.32	32.6 N	68.3 E	18	4.8	P
0900	HIN+011+04AL	1/11/73	4. 4.41	37.0 N	70.0 E	--	3.9	N
0902	AUB+012+17AL	1/12/73	17.35.49	38.0 N	70.0 E	--	3.7	N
0905	KAS+013+01AL	1/13/73	1.53.36	34.0 N	74.0 E	--	3.8	N
0908	SIN+015+12AL	1/15/73	12.55.44	40.4 N	91.1 E	13	5.1	P
0909	SIN+015+14AL	1/15/73	14.42. 7	40.4 N	91.1 E	13	4.7	P
0914	TSI+018+06QD	1/18/73	6.47.28	34.9 N	99.6 E	33	4.6	P
0920	MON+020+01AL	1/20/73	1.50.51	45.0 N	96.0 E	--	3.7	N
0924	KGZ+021+03TD	1/21/73	3.23.53	41.0 N	71.0 E	--	4.3	L
0954	CEN+049+21AL	2/18/73	21.39. 2	40.8 N	74.1 E	33	4.9	P
0955	CEN+050+17AL	2/19/73	17.34.45	32.0 N	88.0 E	--	4.2	N
0965	CEN+054+10AL	2/23/73	10.45. 6	37.6 N	86.4 E	33	4.8	P
0977	CEN+057+18AL	2/26/73	18.34.34	34.0 N	67.0 E	--	3.5	N
1017	CEN+060+12RR	3/ 1/73	12.59.42	42.0 N	97.0 E	--	4.2	L
1033	CEN+062+10AL	3/ 3/73	10.22.46	40.2 N	78.8 E	33	4.6	P
1047	CEN+065+03AL	3/ 6/73	3.30.41	36.0 N	73.0 E	--	3.6	N
1112	CEN+081+01AL	3/22/73	1. 6.57	28.1 N	87.0 E	33	5.2	P
1156	CEN+092+04AL	4/ 2/73	4. 4.33	38.1 N	70.0 E	33	3.8	P
1157	CEN+093+05AL	4/ 3/73	5.50.32	38.0 N	69.0 E	--	3.7	N
1164	CEN+094+17AL	4/ 4/73	17.53. 8	30.5 N	83.7 E	48	4.8	P
1211	CEN+098+03AL	4/ 8/73	3.52.17	38.0 N	75.0 E	--	3.8	N
1219	CEN+103+05AL	4/13/73	6.40.13	36.0 N	73.0 E	--	3.7	N
1220	CEN+103+10AL	4/13/73	10.47.39	33.0 N	86.0 E	--	3.9	N
1241	CEN+111+00AL	4/21/73	0.27.54	36.0 N	77.0 E	--	3.4	N
1246	CEN+113+16AL	4/23/73	16.18.42	28.0 N	93.0 E	--	3.6	N
1263	CEN+120+07AL	4/30/73	7.29.48	50.0 N	89.7 E	33	4.6	P

SECTION III
TCA PROCESSOR GAINS

A. INTRODUCTION

In order to determine TCA processor gains, motion over a 2048 second segment containing a high signal-to-noise ratio ("noise-free") signal as recorded at ALPA was multiplied by a scale factor and added to the noise in a 2048 second segment immediately preceding the signal segment. The TCA processor was then applied to the resulting composite trace. The data were also subjected to a bandpass filter which rejected all energy outside the 0.024-0.059 Hz (17.0-41.5 sec.) passband. A wide range of scale factors was used for each event, so that the composite traces ranged from the case where the signal was completely buried in noise to the case where it was clearly visible. The purpose of this procedure was to determine the dB gain of the TCA processor over the equivalent bandpass filter as the signal emerges from the noise. In particular, we were able through this procedure to make estimates of the dB gain to be expected when the TCA processor is applied to low signal-to-noise ratio events.

Output signal-to-noise ratios were calculated by dividing the maximum zero-to-peak amplitude found within the arrival time window of the processed trace by the root-mean-square (RMS) value of the noise in the time interval prior to the signal arrival. Twenty times the logarithm to the base ten of this quantity is the signal-to-noise ratio:

$$\mathrm{SNR} = 20 \log_{10} \left(\frac{\text{Peak Amplitude}}{\text{RMS Noise}} \right) .$$

Signal-to-noise ratios were calculated for both TCA processed and bandpass filtered traces. The gain of the TCA processor over the equivalent bandpass

filter is the difference between the signal-to-noise ratio of the TCA processor and the equivalent bandpass filter for the same event.

Before proceeding to the determination of dB gain estimates for the TCA processor, one further point must be considered. In the new Love wave TCA processor, some filtering of noise and off-azimuth signals can be performed by requiring that the angle β be less than some limit. (We shall call this limit the β accept-reject limit.) If a value of β greater than this limit is found, it will be assumed that the motion is due to noise or a truly off-azimuth signal. In this case, the real components of the horizontal motion and the imaginary components of the transverse motion will be set to zero. These unwanted components will then not contribute to the TCA-processed motion in the time domain.

The answer to the question of what the β accept-reject limit should be is not immediately obvious. If the limit is set too low, off-azimuth portions of the Love wave (due to scattering and/or multipathing) will be rejected. If this limit is set too high, the desired filtering effect will be weakened.

An empirical solution to this problem was found by selecting several high signal-to-noise ratio events, scaling each signal and adding it to noise so that the true signal-to-noise ratio of the composite trace before processing was 12 dB, and applying the new TCA processor repeatedly while varying the β accept-reject limit from $\pm 5^{\circ}$ to $\pm 90^{\circ}$. The results of this procedure are given in Table III-1.

We see from this table that the dB gain of the Love wave TCA processor over the bandpass filter for two of the test events is highest at 5° and for the other two is highest at 10°. When plots of the data produced by this process were reviewed, it was noted that Love wave energy after the first arrival was increasingly suppressed as the β accept-reject limit was decreased. It was decided that the best tradeoff of maximum dB gain versus

TABLE III-1

dB GAIN OF THE NEW LOVE-WAVE TCA PROCESSOR
OVER THE EQUIVALENT BANDPASS FILTER
AS A FUNCTION OF THE β ACCEPT-REJECT LIMIT

β Limit	dB Gain of New TCA over Bandpass Filter for Test Events			
	Event 172	Event 505	Event 693	Event 1085
$\pm 5^{o}$	10.31	4.56	14.14	7.75
$\pm 10^{o}$	10.46	9.06	7.67	6.92
$\pm 15^{o}$	9.80	6.89	5.64	5.36
$\pm 20^{o}$	10.13	5.95	4.80	5.03
$\pm 25^{o}$	9.03	6.26	3.52	6.13
$\pm 30^{o}$	7.13	5.30	1.81	6.06
$\pm 35^{o}$	7.76	5.12	3.42	5.77
$\pm 40^{o}$	7.34	3.77	3.39	6.67
$\pm 45^{o}$	6.92	3.69	3.14	7.41
$\pm 50^{o}$	5.26	2.98	3.12	6.93
$\pm 55^{o}$	4.15	3.03	3.06	5.24
$\pm 60^{o}$	3.93	2.92	3.09	5.01
$\pm 65^{o}$	3.84	2.45	3.03	1.85
$\pm 70^{o}$	3.48	2.49	2.66	2.08
$\pm 75^{o}$	1.70	-0.17	2.36	2.39
$\pm 80^{o}$	1.71	-0.98	2.36	2.71
$\pm 85^{o}$	0.84	-1.36	0.04	1.92
$\pm 90^{o}$	0.78	-1.25	0.09	2.13

suppression of later Love wave arrivals was at the β accept-reject limit of $\pm 10^{\circ}$. Therefore, all further evaluation of the new Love wave TCA processor will use this value for the β accept-reject limit.

We note that, since only ALPA data was used in this evaluation, it should not be assumed that the above result is applicable to data recorded at other locations.

We shall now turn to the determination of estimates of dB gain due to the TCA processor. In the following figures, which describe the single-site and beam processor gains, the horizontal axis is the true signal-to-noise ratio, in dB, of the composite trace before processing. These values were obtained by multiplying the maximum zero-to-peak signal amplitude by the scale factor mentioned earlier and dividing by the RMS value of the unprocessed composite noise. Twenty times the logarithm of this quantity is the true signal-to-noise ratio.

$$\text{True SNR} = 20 \log \frac{\text{Scale Factor} \cdot \text{Maximum Amplitude}}{\text{RMS Composite Noise}} .$$

The vertical axis is the dB gain of the TCA processed trace over the equivalent bandpass filtered trace at the same scale factor.

We shall review the evaluation of the original TCA processor before considering the results of the new Love wave processor. In order to have our results directly comparable to those published previously (Lane, 1973) we shall use the same test event (KAM-199-08AR, event number 505) as before to evaluate processor gains.

We note one further point before proceeding to the consideration of single-site processor gains. In order to facilitate comparisons between the old and new versions of the TCA processor, it is useful to have one number which represents the dB gain. We propose to use for this the dB gain at 12 dB true signal-to-noise ratio, since we are most interested in the gain we can

expect from the TCA processor for signals at or near the noise level. (A true SNR of 12 dB implies that the maximum signal peak is at or near the amplitude of the maximum noise peak.)

B. SINGLE-SITE PROCESSOR GAINS

Figure III-1 shows the results of applying the original TCA processor to the single-site test event. All three components follow the same general trend. At low true signal-to-noise ratios, where the composite trace is essentially all noise, the gain remains roughly constant. As the true signal-to-noise ratio increases, the gain of the TCA processor over the bandpass filter rises steadily. Finally, at high values of true signal-to-noise ratio, the gain levels off. The important point to note on this figure is that the gain for the Love wave processor does not begin to increase until the true signal-to-noise ratio is much higher than for the Rayleigh wave processor gains. This implies that the original Love wave processor will not be as effective as the Rayleigh wave processor in detecting low signal-to-noise ratio events.

At 12 dB true signal-to-noise ratio, the estimates of dB gain of the original TCA processor are 7.5 dB on the vertical component, 6.5 dB on the transverse component, and 9 dB on the radial component.

Figure III-2 shows the results of applying the new Love wave TCA processor to the single-site test event. The three curves plotted show the dB gain due to rotation about the vertical axis without application of the β accept-reject limit (denoted by a dashed line), the dB gain due to application of the β accept-reject limit without rotation about the vertical axis (denoted by a dotted line), and the dB gain due to application of the β accept-reject limit and rotation about the vertical axis (denoted by a solid line).

This figure shows that simply rotating the data results in a loss in signal-to-noise ratio of 1-2 dB. The explanation for this loss is that the multipathed signal arrives from a restricted range of azimuths, while noise

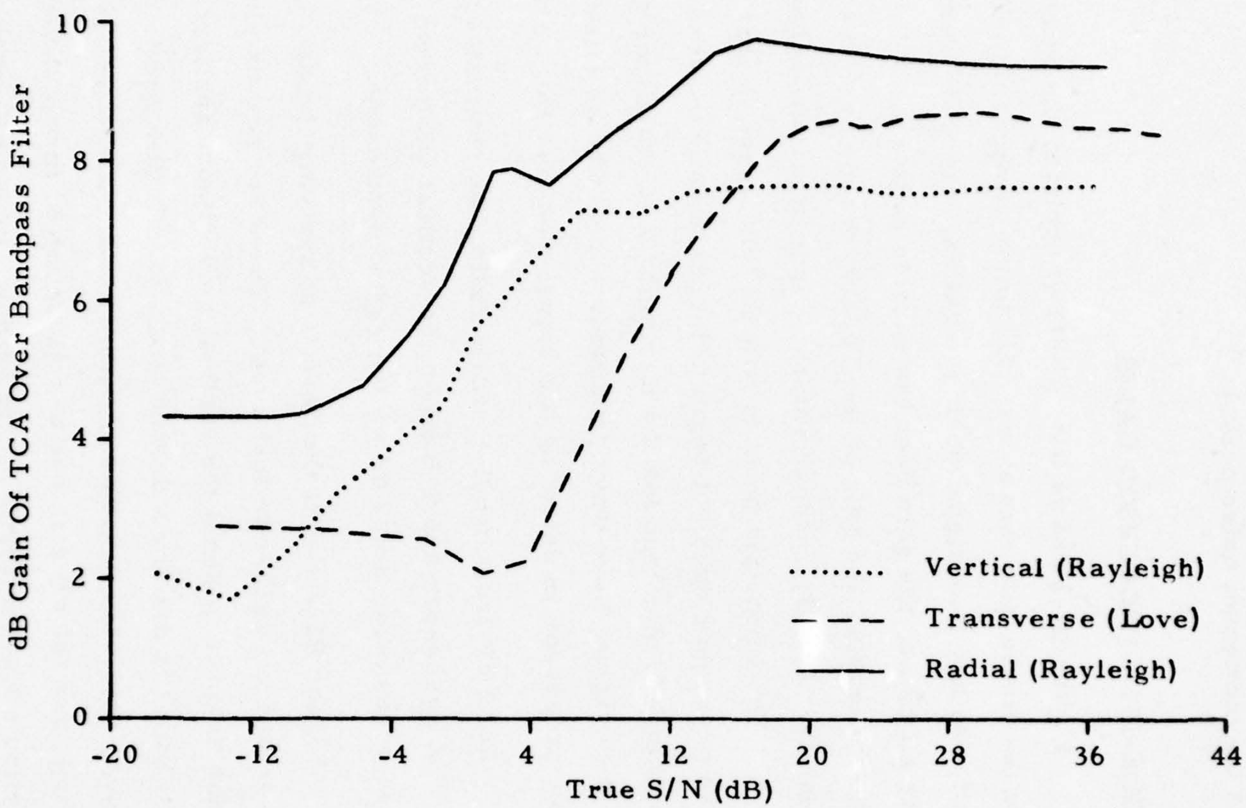

FIGURE III-1

ORIGINAL TCA PROCESSOR - SINGLE SITE DATA
TEST EVENT 505

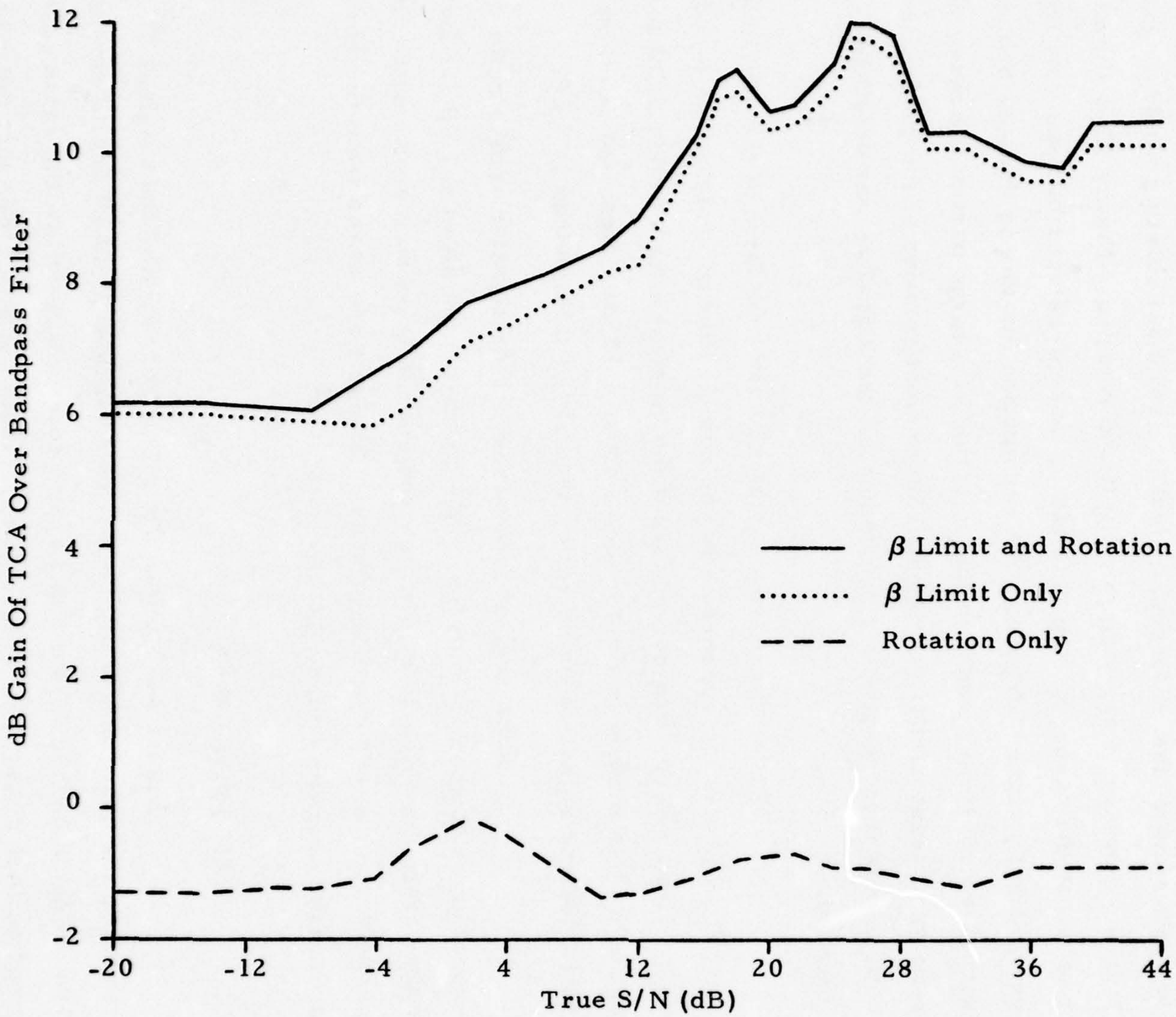

FIGURE III-2

NEW LOVE WAVE TCA - SINGLE SITE DATA
TEST EVENT 505 β LIMIT = 10^{o}

may arrive from any azimuth. Thus, while rotation enhances the signal to some degree, it more greatly enhances the noise, resulting in a lower signal-to-noise ratio. On the basis of the above, one might expect that the gain due to application of the β accept-reject limit and not rotating would be greater than the gain due to applying this limit and rotating. Figure III-2 shows that this is not the case. By applying the β accept-reject limit and rotating, we get a slightly higher dB gain. The explanation for this is that use of the β accept-reject limit results in the rejection of a large part of the noise while passing at least part of the signal. Subsequent rotation of the passed frequency components then results in enhancement of the signal as was originally intended.

From the above, we see that the best form of the new Love wave TCA processor appears to be the combination of applying the β accept-reject limit and rotating by $-\beta$ about the vertical axis. Detection of the signal using this method is first made at about 4 dB true signal-to-noise ratio. At 12 dB true signal-to-noise ratio, the gain of this method is 9 dB.

In summary, at low values of true signal-to-noise ratio we can expect gains of about 7-8 dB for Rayleigh waves and about 6-7 dB for Love waves from the original TCA processor operating on single-site data. In comparison, we can expect gains of about 9 dB for Love waves from the new TCA processor operating on single-site data.

C. BEAM PROCESSOR GAINS

Figure III-3 shows the results of applying the original TCA processor to the beam traces of our test event KAM-199-08AR (event number 505). The dB gains for the vertical and radial components follow the same general trend as they did in the single-site case, with the difference that the rise in gain begins at higher values of true signal-to-noise ratio for the beam data. The dB gain for the transverse component does not show the upward break of

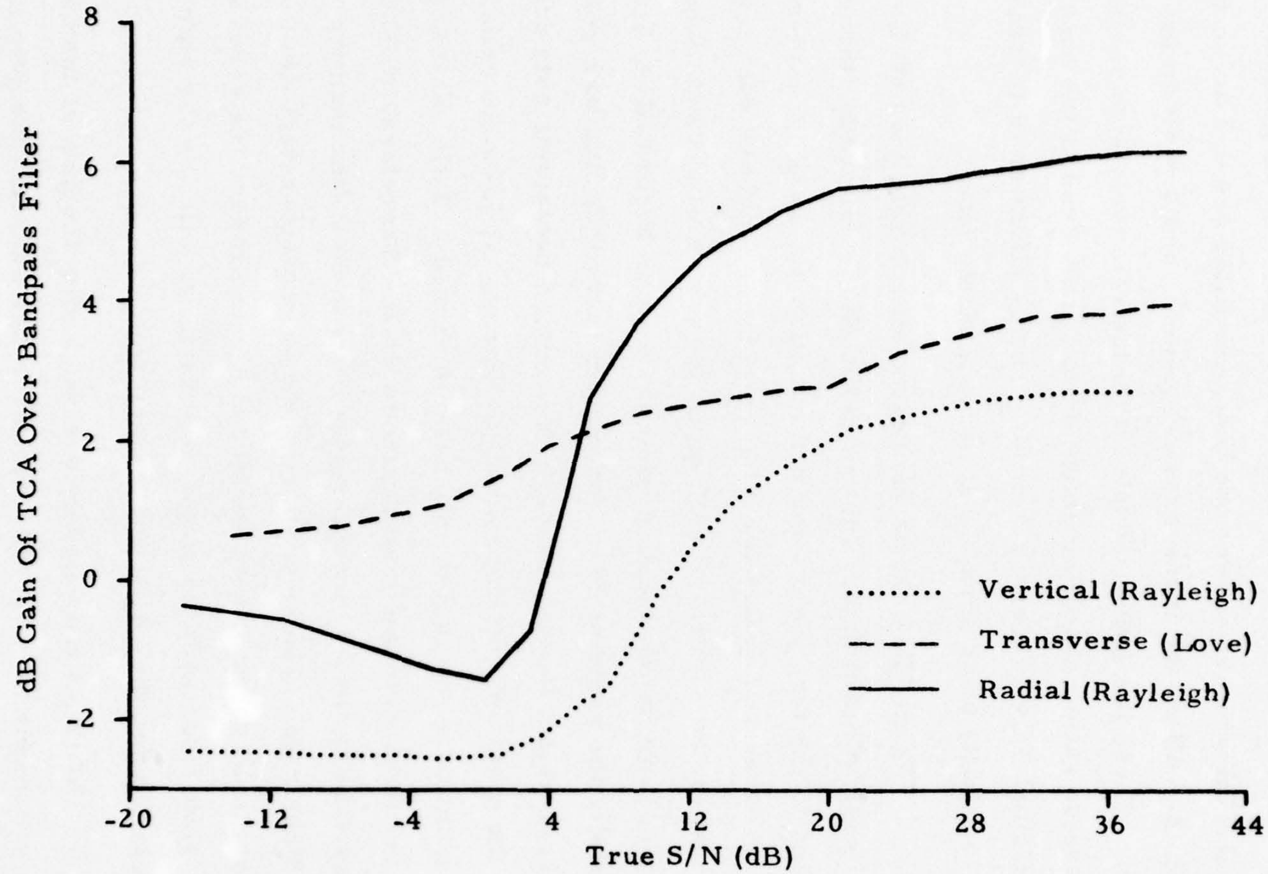

FIGURE III-3

ORIGINAL TCA PROCESSOR - BEAM DATA
TEST EVENT 505

the single-site case, but gradually increases as the true signal-to-noise ratio increases before finally reaching a constant value.

At 12 dB true signal-to-noise ratio, the dB gain estimates of the original TCA processor over the bandpass filter are 0.5 dB on the vertical component, 2.5 dB on the transverse component, and 4.5 dB on the radial component. These low gains, coupled with the relatively high values of true signal-to-noise ratio needed for detection to occur, lead to the conclusion that the original TCA processor should not be as effective in increasing the detection capability of an array as it is for a single site.

Figure III-4 shows the results of applying the new Love wave TCA processor to beam data. Just as in the single-site case, three versions were applied to the test event: one with rotation but no β accept-reject limit, one with the β accept-reject limit but no rotation, and one with rotation and the β accept-reject limit. The dB gains for the version containing the β accept-reject limit but no rotation are not shown in Figure III-4, since they are essentially the same as those for the version containing both rotation and the β accept-reject limit. Although the version containing only rotation outperforms the other two versions at 12 dB true signal-to-noise ratio, we note that at no point does the gain of this version exceed 0.5 dB, whereas both the other two versions have maximum gains of 4 dB. Therefore, we judge the versions containing the β accept-reject limit to be better than the version without. Since both versions containing the β accept-reject limit yield essentially the same dB gains, we can select either to process the event suites. To facilitate comparison with the single-site data, we will use the version containing both rotation and the β accept-reject limit.

At 12 dB true signal-to-noise ratio, the gain of the new Love wave TCA processor is -1.5 dB. However, we note that the gain is rising rapidly at 12 dB true signal-to-noise ratio, reaching approximately 2 dB at 16

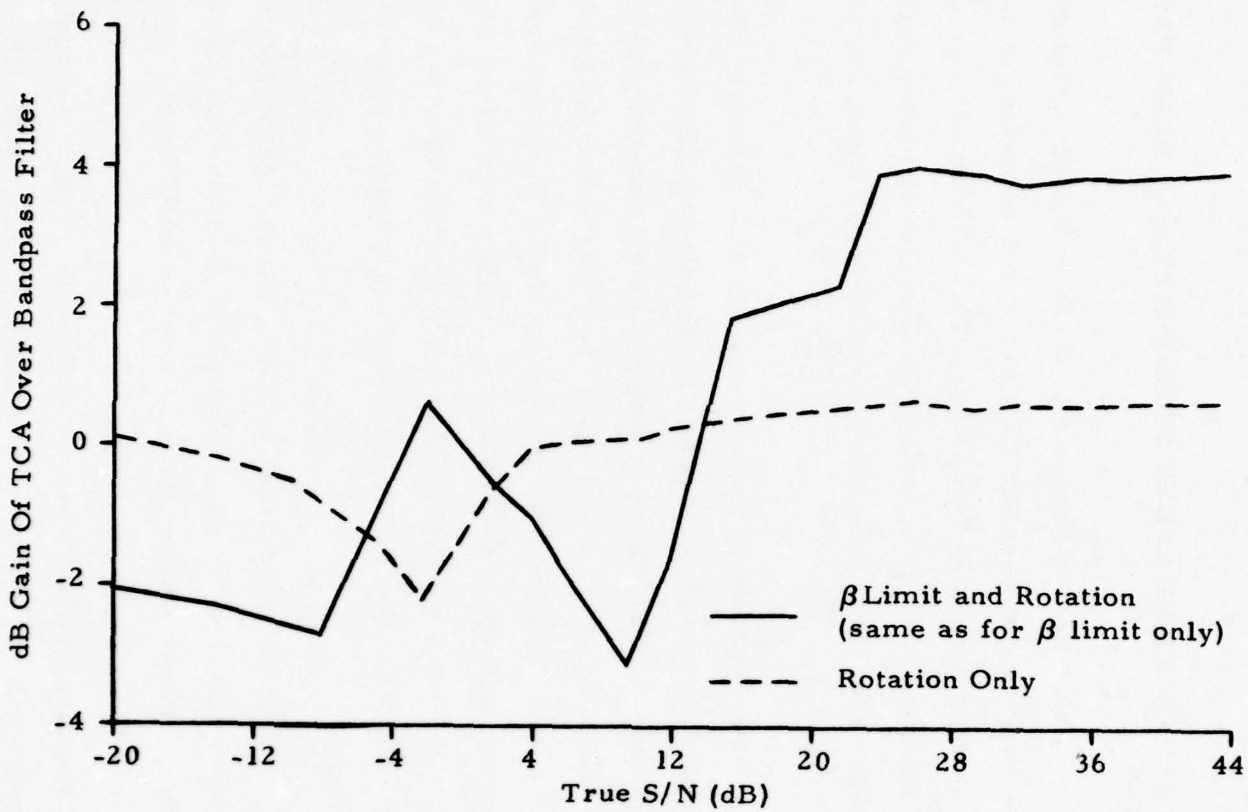

FIGURE III-4

NEW LOVE WAVE TCA - BEAM DATA
TEST EVENT 505 β LIMIT = 10^{o}

dB true signal-to-noise ratio. Therefore, in the beam data case, we can expect little if any improvement in detection capability from either the original or new TCA processors.

D. DIFFERENCES BETWEEN SINGLE-SITE AND BEAM PROCESSOR GAINS

Table III-2 indicates that there is a great difference between the gains we may expect when the TCA processor is applied to single-site data and when it is applied to beam data. This difference in performance implies some inherent difference between single-site and beam data due to beamforming. This difference may lie either in the noise, in the signal, or in both.

As recorded at an individual station, the noise field consists of non-propagating noise and propagating noise with the characteristics of surface waves. The beamforming process suppresses the non-propagating noise by a factor approximately equal to the square root of the number of stations in the array. The amount by which the propagating noise is suppressed is dependent upon the arrival azimuth of this noise; the farther it is off the beam azimuth, the more it will be suppressed. Thus, after beamforming the noise will have a relatively larger component of on-azimuth propagating noise than before beamforming.

Now let us consider how the TCA processor acts on noise. The TCA processor searches for particular phase relationships among the components of motion. These relationships will not be found (except possibly at isolated points) in the non-propagating noise, since in this type of noise they are random. They also will not be found in the off-azimuth propagating noise, since this noise will not appear on the proper components. The TCA processor will, however, pass the on-azimuth propagating noise, since in this case the phase relationships will be correct.

TABLE III-2

SUMMARY OF GAIN ESTIMATES

Component	Gain in dB	
	Single Site	Beam
Original TCA-LR-V	7.5	0.5
Original TCA-LQ-T	6.5	2.5
Original TCA-LR-R	9.0	4.5
New TCA-LQ-T	9.0	-1.5

Thus we see that the beamforming process passes the same on-azimuth propagating noise. We cannot, therefore, expect any appreciable gain when we apply the TCA processor to beam data, since the type of noise it can suppress has already been suppressed in beamforming.

We shall now consider whether the difference between single-site and beam processor gains may be due to some difference between the single-site and beam signals. Before the beam is formed from the individual sites, differences in arrival time at each of the sites (delay times) are computed. The signal recorded at each site is then time-shifted by these delay times to time-align the signals, which are then added and scaled. If the delay times are in error, due to improper location of the event epicenter, the phase relationships between the components of motion will be distorted, resulting in a loss in signal amplitude when later processed by the TCA processor. If this is the case, we should see greater suppression of the beam signal than the single-site amplitude on the TCA processor output.

Table III-3 breaks down the dB gain estimates of Table III-2 into the gain due to noise suppression and the gain due to signal suppression. The gain due to noise suppression is the difference between the RMS noise in dB of the trace before TCA processing and the RMS noise in dB of the trace after processing. The gain due to signal suppression is the ratio, expressed in dB, of the peak signal amplitude measured after TCA processing to the peak signal amplitude measured before TCA processing. The net gain is then simply the sum of the gain due to noise suppression and the gain due to signal suppression.

This table shows clearly that the differences between single-site and beam processor gains are due to differences in the amount of noise suppression and to differences in signal suppression.

TABLE III-3

GAIN ESTIMATES AT 12 dB TRUE SIGNAL-TO-NOISE
(FROM TEST EVENT 505)

Component	Single Site / Beam	Gain in dB due to Noise Suppression	Gain in dB due to Signal Suppression	Net Gain in dB
Original TCA LR-V	Single Site	8.7	-1.2	7.5
	Beam	5.3	-4.8	0.5
Original TCA LQ-T	Single Site	10.2	-3.7	6.5
	Beam	6.4	-3.9	2.5
New TCA LQ-T	Single Site	12.2	-3.2	9.0
	Beam	4.7	-6.2	-1.5
Original TCA LR-R	Single Site	11.2	-2.2	9.0
	Beam	7.9	-3.4	4.5

SECTION IV
DETECTION CAPABILITY ESTIMATES

A. INTRODUCTION

Before processing the event suites with the new Love wave TCA processor, it was necessary to check our definitions of detection criteria. Therefore, we processed twenty noise samples with this method. The output showed that TCA processed noise tends to be predominantly 18-20 second period energy with packets of lower frequency energy appearing as the β accept-reject limit increases. Signal-like packets were occasionally found; however, these did not display dispersion and changed only slightly as the β accept-reject limit was increased. In contrast to this, it was noticed that signals appear to 'grow' as the β accept-reject limit increases, indicating the inclusion of more off-azimuth (multipath) energy.

From the above, it is obvious that the principal detection criterion remains the presence of dispersion in the signal gate. Other detection criteria are that the suspected signal begins close to its predicted arrival time and that the largest peak of the suspected signal be 3 dB or more above any other peak in a gate starting 100 seconds before the estimated signal arrival time and ending 100 seconds after the estimated signal end time. (This last criterion should not be considered to be absolute. It is occasionally possible to detect a signal from its dispersion characteristics even though its largest peak amplitude is equal to that of the largest noise peaks.)

All events listed in Tables II-1 and II-2 were processed by the new Love wave TCA processor and evaluated with the above detection criteria

to determine the improvement in detection capability due to this method. In addition, since only a small suite of events was used in the original TCA evaluation (Lane, 1973) and since we wish to make direct comparisons between the original and new Love wave TCA processors, both event suites were also processed by the original method. The version of the new Love wave TCA processor used here is the one with rotation and the β accept-reject limit, since in Section III we found that this version yielded higher dB gains than the version which contained only rotation or the version which contained only the β accept-reject limit.

B. SINGLE-SITE DATA RESULTS

We will consider detection capability improvement for single-site data in terms of the fifty percent detection threshold and in terms of the change in the number of events detected. The fifty percent detection threshold is defined as the m_b value at which the probability of detecting an event is fifty percent. We will not discuss detection capability improvement for the radial component, since results for this component are essentially identical to those for the vertical component. Figures B-1 to B-5 of Appendix B present the detection statistics for the 86 events of the southern Kamchatka suite. Figures B-6 to B-10 present the detection statistics for the 76 events of the central Asia suite. These detection statistics are summarized in Table IV-1.

From Table IV-1, we see that the Rayleigh wave part of the original TCA processor yielded a fifty percent detection threshold improvement of 0.41 m_b units for the southern Kamchatka event suite and 0.24 m_b units for the central Asia event suite. These correspond to processor gains of approximately 8 dB and 5 dB, respectively. These values compare fairly well with the 7.5 dB gain estimate made in Section III. The Love wave part of the original TCA processor yielded a fifty percent detection threshold improvement of 0.17 m_b units for the southern Kamchatka event suite and 0.25 m_b units for the

TABLE IV-1

SUMMARY OF 50 PERCENT DETECTION THRESHOLD ESTIMATES IN m_b UNITS

Type of Estimate	Region	
	Southern Kamchatka	Central Asia
LR-V Bandpass	4.61	4.59
LQ-T Bandpass	4.49	4.73
LR-V Original TCA	4.20	4.35
LQ-T Original TCA	4.32	4.48
LQ-T New TCA	4.11	4.38

central Asia event suite. These correspond to processor gains of approximately 3.5 dB and 5 dB, respectively. These values compare fairly well with the 6.5 dB gain estimate made in Section III.

Table IV-1 shows that the new Love wave TCA processor (rotation and β accept-reject limit) yielded a fifty percent detection threshold improvement of about 0.35 m_b units for both regions, corresponding to a processor gain of 7 dB. This compares quite well with the 9 dB gain estimate made in Section III.

Another way of viewing the detection capability improvement of the TCA processor is to consider the number of events detected on the processor output which were not detected on the bandpass filter output. These results are summarized in Table IV-2. From this data we see that the Rayleigh wave part of the original TCA processor and the new Love part of the TCA processor perform somewhat better on the southern Kamchatka data than on the central Asia data. The original Love wave part of the TCA processor performs equally well on data from the two regions. In agreement with previous results, we see that the new Love wave part of the TCA processor is superior in performance to the original Love wave part.

The data listed in Table IV-2 indicate that both the original Rayleigh wave processor and the new Love wave processor can be expected to detect approximately 20 to 35 percent of those events not detected on the bandpass filter output. This, of course, assumes that the original data base has m_b and detection/non-detection distributions similar to the data bases used in this evaluation.

C. BEAM DATA RESULTS

The results reported by Lane (1973) and the results of Section III of this report all indicate that the TCA processor in both its original and new forms is of little value when applied to beam data. For the sake of

TABLE IV-2

TCA PROCESSOR NET GAIN IN DETECTION - SINGLE-SITE DATA

Detection Status	Southern Kamchatka		Central Asia	
	Number	Percentage	Number	Percentage
Events not detected on LR-V BP	60	--	54	--
Events not detected on LQ-T BP	57	--	58	--
Detections on Original LR-V TCA	17	28%	11	20%
Detections on Original LQ-T TCA	9	16%	11	19%
Detections on new LQ-T TCA	20	35%	14	24%

thoroughness, however, the beams of the central Asia suite of events were processed in the same manner as the single-site data. The results of this processing are shown in Figures B-11 to B-15 of Appendix B and summarized in Table IV-3. These results simply reconfirm previous results. The only significant improvement in detection capability was made on the LR-V part of the TCA processor. This 0.15 m_b unit lowering of the fifty percent detection threshold, in conjunction with the insignificant changes in detection threshold due to either form of the Love wave TCA processor, indicate that it would not be productive to routinely apply the TCA processor to beam data.

TABLE IV-3

SUMMARY OF 50 PERCENT DETECTION THRESHOLD ESTIMATES
BEAM DATA IN m_b UNITS

Type of Estimate	50% Detection Threshold
LR-V Bandpass	4.27
LQ-T Bandpass	4.31
LR-V Original TCA	4.12
LQ-T Original TCA	4.24
LQ-T New TCA	4.27

SECTION V
CONCLUSIONS

The following results have been found during the course of this evaluation of the Three-Component Adaptive (TCA) processor:

- The most effective form of the new Love wave TCA processor contains rotation of the Love wave frequency components about the vertical axis to the transverse component with an accept-reject limit placed on the Love wave arrival azimuth.
- At 12 dB true signal-to-noise ratio, we can expect 7-9 dB gain for Rayleigh waves and 6-7 dB gain for Love waves from the original TCA processor on single-site data.
- At 12 dB true signal-to-noise ratio, we can expect about 9 dB gain for Love waves from the new TCA processor on single-site data.
- Only low or negative gains can be expected from either version of the TCA processor when applied to beam data.
- Use of the original TCA processor on single-site data lowered the fifty percent Rayleigh wave detection threshold by about 0.25-0.4 m_b units and the fifty percent Love wave detection threshold by about 0.15 m_b units.
- Use of the new Love wave TCA processor on single-site data lowered the fifty percent Love wave detection threshold by about 0.35 m_b units.

- Use of the original TCA processor on beam data yielded a small (0.15 m_b unit) improvement in the Rayleigh wave fifty percent detection threshold and essentially no change in the Love wave fifty percent detection threshold.
- Use of the new Love wave TCA processor on beam data yielded essentially no change in the Love wave fifty percent detection threshold.

The above points make it clear that the original Rayleigh wave TCA processor and the new Love wave TCA processor are effective when applied to single-site data. No version is effective when applied to beam data.

SECTION VI
REFERENCES

Lambert, D. G., A. I. Tolstoy, and E. S. Becker, 1974, Seismic Detection and Discrimination Capabilities of the Very Long Period Experiment - Final Report; Technical Report No. 7, Texas Instruments Report No. ALEX(01)-TR-74-07, AFTAC Contract Number F08606-74-C-0033, Texas Instruments Incorporated, Dallas, Texas.

Lane, S. S., 1973, Evaluation of an Adaptive Three-Component Filter; Special Report No. 15, Texas Instruments Report No. ALEX(01)-STR-73-15, AFTAC Contract Number F33657-72-C-0725, Texas Instruments Incorporated, Dallas, Texas.

Shimshoni, M., and S. W. Smith, 1964, Seismic Signal Enhancement With Three-Component Detectors, Geophysics, 29, 664.

Strauss, A. C., 1973, Final Evaluation of the Detection and Discrimination Capability of the Alaskan Long Period Array; Special Report No. 8, AFTAC Contract Number F33657-72-C-0725, Texas Instruments Incorporated, Dallas, Texas.

Strauss, A. C., and A. I. Tolstoy, 1974, Evaluation of Matched Filters and the Three-Component Adaptive Processor for the VLPE Stations and VLPE Network; Technical Report No. 5, Texas Instruments Report No. ALEX(01)-TR-74-05, AFTAC Contract Number F08606-74-C-0033, Texas Instruments Incorporated, Dallas, Texas.

APPENDIX A
THE UPGRADE TCA PROGRAM

The program listing given on the following pages is the most general version available. It will work on either single-site or beam data and can be used to determine processor gains or to enhance detection studies. To use this program, note the following data card inputs:

DATA CARD INPUT

Card	Column	Format	Parameter
1	1-12	3A4	Event name to be processed
1	21-22	I2	Vertical Trace Number
1	23-24	I2	Transverse Trace Number
1	25-26	I2	Radial Trace Number
2	5	I1	ISUM. If ISUM= 0, process entire trace. If ISUM≠ 0, scale second half of trace and add to first half.
	6-15	F10.3	SCFAC - factor with which to scale second half of trace (used if ISUM ≠ 0).
	16-25	F10.4	FLO - low frequency of bandpass filter
	26-35	F10.4	FHI - high frequency of bandpass filter
	36-45	F10.2	ANGBET - accept/reject limit for Love wave arrival azimuth
	50	I1	IFLAG. If IFLAG= 0, process single-site data; if IFLAG≠ 0, process beam data.

In general, the trace numbers used on card one are as follows:

Trace 1 - vertical single-site data

Trace 2 - transverse single-site data

Trace 3 - radial single site data

Trace 4 - vertical beam data (NORSAR);
transverse beam data (ALPA)

Trace 5 - transverse beam data (NORSAR);
vertical beam data (ALPA)

Trace 6 - radial beam data

Input Tape - TDFILTER beam tape; mounted on SYS018

Output Plot Tape - Scratch tape mounted on SYS006

Restrictions:

All three components must be available.

Data length must be a power of two.

MAIN PROGRAM
(PAGE 1 OF 2)

```
      DIMENSION EHEAD(400),BEEM(2100,3),IEHEAD(400)
      DIMENSION EVENT(3),THEAD(40)
      DIMENSION DTYPE(2)
      DIMENSION EOI(20)
      INTEGER*2 TAPENO(3)
      INTEGER BEAMNO(3)
      EQUIVALENCE (TAPENO,THEAD(2))
      EQUIVALENCE (EHEAD,IEHEAD)
      DATA DTYPE/'TDBE','AM  '/
      DATA EOI/'EOI0',19*'    '/
C
      ITRACK(J)=3*(J-1)+2
      IU=18
      CALL TIDISK('OPEN')
      CALL TIOPEN(IU,THEAD,&9999)
      WRITE(3,50) THEAD
   50 FORMAT(/////20X,'INPUT TAPE LABELS ARE'//,2(10X,1H',20A4,1H',/))
C
C     READ CONTROL CARDS
C
  100 READ(1,110,END=9998) EVENT,(BEAMNO(I),I=1,3)
  110 FORMAT(3A4,8X,3I2)
      WRITE(3,120) EVENT
  120 FORMAT(1H1,10X,'EVENT NAME = ',1H',3A4,1H')
      CALL TIINTP('INPUT','SEARCH',IU,IEHEAD,EVENT,IC)
      IF(IC.EQ.0) GO TO 130
      WRITE(3,126) IC
  126 FORMAT(10X,'TIINTP ERROR CODE = ',Z8)
      WRITE(3,125) EVENT
  125 FORMAT(1H1,10X,'EVENT ',1H',3A4,' NOT FOUND--ABORT')
      GO TO 9998
  130 CALL DISKIO('WRIT',1,IEHEAD,340,&100)
      WRITE(3,121) BEAMNO(1),BEAMNO(2),BEAMNO(3)
  121 FORMAT(10X,'BEAMS TO PROCESS (V,T,R) = ',3I2)
      CALL LSHEAD(4,IEHEAD)
      NBEEMS=IEHEAD(29)
      TIMES=IEHEAD(46)
      NBYT=IEHEAD(8)
      LEN=(NBYT/4)-25
      TIMEL=IEHEAD(68)-IEHEAD(46)
      TIMER=IEHEAD(70)-IEHEAD(46)
      TIMEE=TIMER+IEHEAD(73)
```

```
C
C      READ INPUT DATA FROM TAPE AND PUT ON DISK
C
       DO 220 I=1,NBEEMS
       CALL TIREAD(IU,BEEM,NBYT,IC,&160,&180,&160)
       CALL DISKIO('WRIT',ITRACK(I),BEEM,NBYT/4,&200)
       GO TO 220
  160  WRITE(3,170) I,IC
  170  FORMAT(/2X,'TAPE ERROR ON BEAM NUMBER =',I5,5X,'IC=',Z8)
       GO TO 220
  180  WRITE(3,190) I
  190  FORMAT(//5X,'BEAM NUMBER =',I3,' NOT FOUND')
       GO TO 220
  200  WRITE(3,210) I
  210  FORMAT(//5X,'DISK ERROR ON WRITE INDEX =',I3,//)
  220  CONTINUE
C
       DO 270 K=1,3
       DO 230 I=1,2100
  230  BEEM(I,K)=0.0
       NUMBEM=BEAMNO(K)
       IF(NUMBEM.LE.NBEEMS) GO TO 240
       WRITE(3,190) NUMBEM
       GO TO 270
  240  CALL DISKIO('READ',ITRACK(NUMBEM),BEEM(1,K),NBYT/4,&250)
       GO TO 270
  250  WRITE(3,260) K,NUMBEM
  260  FORMAT(//5X,'DISK ERROR ON READ.  LOOP=',I3,'  NUMBEM=',I3//)
  270  CONTINUE
       CALL LHOADL(BEEM,LEN,EVENT,TIMES,TIMEL,TIMER,TIMEE)
       GO TO 100
 9998  CALL TIDISK('CLOS')
       CALL PLOT(0.0,0.0,999)
 9999  CALL TITAPE('UNLOAD',IU,BEEM,NBYTE,IC)
       STOP
       END
```

```
      SUBROUTINE LHQADL(DATA,NTDIM,NAME,TIMES,TIMEL,TIMER,TIMEE)
      DIMENSION F(3),TEMP(3),DATA(2100,3),PROC(2100,3),IBIT(512)
      DIMENSION TRG(512),IIBIT(512),TRIG(512),PBUF(64,3,2)
      DIMENSION FIN(2100,3),TSQD(3),CTIME(3),NAME(1),ASK(20)
      DATA ASK/20*'****'/
      IPTSEG=64
      IPOWER=3
 100  CALL PLOT (0.0,-12.0,-3)
      CALL PLOT (0.0,10.0,-3)
      CALL PLOT (0.,-0.5,-3)
C
C          ISUM EQ 0     PROCESS ENTIRE TRACE
C          ISUM NE 0     SCALE SECOND HALF OF TRACE AND ADD TO FIRST HALF
C          SCFAC IS THE SCALE FACTOR FOR THE SIGNAL HALF OF THE TRACE
C          IF ISUM = 0, SCFAC MUST = 1.0
C          FLO = LOW BANDPASS FREQUENCY
C          FHI = HIGH BANDPASS FREQUENCY
C          ANGBET = ACCEPT/REJECT LIMIT ON BETA
C          IFLAG EQ 0     SINGLE SITE DATA
C          IFLAG NE 0     BEAM DATA
C          TAPR = AMOUNT OF BP FILTER TAPER--MAY NOT BE ZERO
C
      READ(1,110,END=9998) ISUM,SCFAC,FLO,FHI,ANGBET,IFLAG,TAPR
  110 FORMAT(I5,F10.3,F10.4,F10.4,F10.2,I5,F10.4)
      CALL SYMBOL(0.0,-2.0,0.2,'EVENT NAME',0.0,10)
      CALL SYMBOL(0.0,-3.0,0.2,'START TIME',0.0,10)
      CALL SYMBOL(0.0,-4.0,0.15,'LOW BP FREQ',0.0,11)
      CALL SYMBOL(0.0,-4.5,0.15,'HIGH BP FREQ',0.0,12)
      CALL NUMBER(2.5,-4.5,0.15,FHI,0.0,4)
      CALL NUMBER(2.5,-4.0,0.15,FLO,0.0,4)
      CALL NUMBER(2.5,-3.0,0.2,TIMES,0.0,-1)
      CALL SYMBOL(2.5,-2.0,0.2,NAME,0.0,12)
      IF(IFLAG.NE.0) GO TO 115
      CALL SYMBOL(0.0,-5.0,0.15,'SINGLE SITE DATA',0.0,16)
      GO TO 117
  115 CALL SYMBOL(0.0,-5.0,0.15,'BEAM DATA',0.0,9)
  117 IF(ISUM.EQ.0) GO TO 120
      CALL SYMBOL(0.0,-5.5,0.15,'SIGNAL S.F.',0.0,11)
      CALL NUMBER(2.5,-5.5,0.15,SCFAC,0.0,4)
  120 CALL PLOT(12.0,1.4,-3)
C
C     SCALE SIGNAL AND ADD TO PRECEEDING NOISE, IF DESIRED
C
      IF(ISUM.EQ.0) GO TO 215
      TIMEL=TIMEL-NTDIM
      TIMER=TIMER-NTDIM
      TIMEE=TIMEE-NTDIM
      CALL SCALAD(DATA,PROC,NTDIM,SCFAC,TIMEL)
      GO TO 214
  215 DO 210 J=1,3
      DO 210 I=1,NTDIM
  210 PROC(I,J)=DATA(I,J)
```

SUBROUTINE LHQADL
(PAGE 2 OF 5)

```
C
C      COMPUTE AND PRINT OUT COMPOSITE S/N RATIOS
C
  214 CALL RMS(PROC,CTIME,TSGD,TIMEL,TIMEE,F,TEMP,ISUM)
      WRITE(3,216)(ASK(I),I=1,20)
  216 FORMAT(15X,20A4)
      WRITE(3,211) FLO,FHI,TAPR
  211 FORMAT(10X,'***** FLO = ',F7.4,'  **  FHI = ',F7.4,'  **  TAPER =
     1',F7.4,'  *****')
      IF(ISUM.EQ.0) GO TO 219
      WRITE(3,217)
  217 FORMAT(5X,'          ')
      WRITE(3,218) SCFAC
  218 FORMAT(35X,'SIGNAL SCALING FACTOR = ',F7.5)
      WRITE(3,217)
  219 WRITE(3,220)
  220 FORMAT(20X,'UNPROCESSED DATA')
      WRITE(3,230)
  230 FORMAT(20X,'S/N',12X,'AT TIME',8X,'RMS NOISE',10X,'PEAK')
      WRITE(3,240)(TSGD(J),CTIME(J),F(J),TEMP(J),J=1,3)
  240 FORMAT(20X,F6.2,9X,F6.0,10X,F5.2,10X,E10.3/,20X,F6.2,9X,F6.0,10X,F
     15.2,10X,E10.3/,20X,F6.2,9X,F6.0,10X,F5.2,10X,E10.3)
      WRITE(3,217)
C
C      PERFORM THREE-COMPONENT ADAPTIVE PROCESSING
C
      DO 260 J=1,3
      DO 250 I=1,IPTSEG
  250 PBUF(I,J,1)=PROC(I,J)
  260 CALL TIDFFT(PBUF(1,J,1),TRG,IBIT,IPTSEG)
      CALL LOVFIL(PBUF,IPTSEG,ANGBET)
      CALL RAYFIL(PBUF,IPTSEG,IPOWER)
      DO 330 J=1,3
  330 CALL TIIFFT(PBUF(1,J,1),TRIG,IIBIT,IPTSEG)
      I02=IPTSEG/2
      DO 340 J=1,3
      DO 340 I=1,I02
  340 FIN(I,J)=PBUF(I,J,1)
      INTDO=(NTDIM/IPTSEG)*2-2
      NCOUNT=I02
      DO 450 KKK=1,INTDO
      DO 350 J=1,3
      DO 350 I=1,IPTSEG
      PBUF(I,J,2)=PBUF(I,J,1)
  350 PBUF(I,J,1)=PROC(I+NCOUNT,J)
      DO 360 J=1,3
  360 CALL TIDFFT(PBUF(1,J,1),TRG,IBIT,IPTSEG)
      CALL LOVFIL(PBUF,IPTSEG,ANGBET)
      CALL RAYFIL(PBUF,IPTSEG,IPOWER)
      DO 430 J=1,3
  430 CALL TIIFFT(PBUF(1,J,1),TRIG,IIBIT,IPTSEG)
```

```
      EI02=I02
      DO 440 I=1,I02
      ECOUNT=I
      RAT=ECOUNT/EI02
      DO 440 J=1,3
  440 FIN(I+NCOUNT,J)=PBUF(I,J,1)*RAT+PBUF(I+I02,J,2)*(1.0-RAT)
  450 NCOUNT=NCOUNT+I02
C
C     BANDPASS FILTER THE ADAPTIVE-PROCESSED TRACES
C
      DO 460 J=1,3
      DO 460 I=1,I02
  460 FIN(I+NCOUNT,J)=PBUF(I+I02,J,1)
      DO 470 J=1,3
  470 CALL TIDFFT(FIN(1,J),TRIG,IBIT,NTDIM)
      CALL FILTBP(FIN,NTDIM,FLO,FHI,TAPR)
      DO 500 J=1,3
  500 CALL TIIFFT(FIN(1,J),TRIG,IIBIT,NTDIM)
C
C     COMPUTE AND PRINT OUT ADAPTIVE S/N RATIOS
C
      CALL RMS(FIN,CTIME,TSQD,TIMEL,TIMEE,F,TEMP,ISUM)
      WRITE(3,510)
  510 FORMAT(20X,'TCA PROCESSED DATA')
      WRITE(3,230)
      WRITE(3,240)(TSQD(J),CTIME(J),F(J),TEMP(J),J=1,3)
      WRITE(3,515) ANGBET
  515 FORMAT(15X,'***** LQ-T ACCEPT/REJECT LIMIT ON BETA = ',F6.2,' DEGR
     1EES *****')
C
C     PLOT TCA PROCESSED TRACES
C
      CALL SYMBOL(-3.0,-1.0,0.2,'VERTICAL ADAPT',0.0,14)
      CALL SYMBOL(-3.0,-1.6,0.15,'S/N',0.0,3)
      CALL NUMBER(-2.0,-1.6,0.15,TSQD(1),0.0,2)
      CALL SYMBOL(-3.0,-1.9,0.15,'AT TIME',0.0,7)
      CALL NUMBER(-1.0,-1.9,0.15,CTIME(1),0.0,-1)
      CALL PLOT(0.0,0.0,3)
      CALL PLTRTN(FIN(1,1),NTDIM,2.0,TIMEL,TIMER,TIMEE,SF)
      CALL SYMBOL(-3.0,0.3,0.15,'S.F.',0.0,4)
      CALL NUMBER(-2.4,0.3,0.15,SF,0.0,6)
      CALL PLOT(0.0,0.0,3)
      CALL SYMBOL(-3.0,-1.0,0.2,'TRANSVERSE ADAPT',0.0,16)
      CALL SYMBOL(-3.0,-1.6,0.15,'S/N',0.0,3)
      CALL NUMBER(-2.0,-1.6,0.15,TSQD(2),0.0,2)
      CALL SYMBOL(-3.0,-1.9,0.15,'AT TIME',0.0,7)
      CALL NUMBER(-1.0,-1.9,0.15,CTIME(2),0.0,-1)
      CALL PLOT(0.0,0.0,3)
      CALL PLTRTN(FIN(1,2),NTDIM,2.0,TIMEL,TIMER,TIMEE,SF)
      CALL SYMBOL(-3.0,0.3,0.15,'S.F.',0.0,4)
```

SUBROUTINE LHQADL
(PAGE 4 OF 5)

```
      CALL NUMBER(-2.4,0.3,0.15,SF,0.0,6)
      CALL PLOT(0.0,0.0,3)
      CALL SYMBOL(1.0,0.2,0.1,'BETA ACCEPT-REJECT LIMIT EQUALS',0.0,31)
      CALL NUMBER(4.2,0.2,0.1,ANGBET,0.0,2)
      CALL PLOT(0.0,0.0,3)
      CALL SYMBOL(-3.0,-1.0,0.2,'RADIAL ADAPT',0.0,12)
      CALL SYMBOL(-3.0,-1.6,0.15,'S/N',0.0,3)
      CALL NUMBER(-2.0,-1.6,0.15,TSQD(3),0.0,2)
      CALL SYMBOL(-3.0,-1.9,0.15,'AT TIME',0.0,7)
      CALL NUMBER(-1.0,-1.9,0.15,CTIME(3),0.0,-1)
      CALL PLOT(0.0,0.0,3)
      CALL PLTRTN(FIN(1,3),NTDIM,2.0,TIMEL,TIMER,TIMEE,SF)
      CALL SYMBOL(-3.0,0.3,0.15,'S.F.',0.0,4)
      CALL NUMBER(-2.4,0.3,0.15,SF,0.0,6)
      CALL PLOT(0.0,0.0,3)
C
C     BANDPASS FILTER THE COMPOSITE TRACES
C
      DO 520 J=1,3
      DO 520 I=1,NTDIM
  520 FIN(I,J)=PROC(I,J)
      DO 530 J=1,3
  530 CALL TIDFFT(FIN(1,J),TRG,IBIT,NTDIM)
      CALL FILTBP(FIN,NTDIM,FLO,FHI,TAPR)
      DO 560 J=1,3
  560 CALL TIIFFT(FIN(1,J),TRIG,IIBIT,NTDIM)
C
C     COMPUTE AND PRINT OUT BANDPASS S/N RATIOS
C
      CALL RMS(FIN,CTIME,TSQD,TIMEL,TIMEE,F,TEMP,ISUM)
      WRITE(3,570)
  570 FORMAT(20X,'BANDPASS FILTERED DATA')
      WRITE(3,230)
      WRITE(3,240)(TSQD(J),CTIME(J),F(J),TEMP(J),J=1,3)
      CALL SYMBOL(-3.0,-1.0,0.2,'VERTICAL BP FILT',0.0,16)
      CALL SYMBOL(-3.0,-1.6,0.15,'S/N',0.0,3)
      CALL NUMBER(-2.0,-1.6,0.15,TSQD(1),0.0,2)
      CALL PLOT(0.0,0.0,3)
      CALL PLTRTN(FIN(1,1),NTDIM,2.0,TIMEL,TIMER,TIMEE,SF)
      CALL SYMBOL(-3.0,0.3,0.15,'S.F.',0.0,4)
      CALL NUMBER(-2.5,0.3,0.15,SF,0.0,6)
      CALL PLOT(0.0,0.0,3)
      CALL SYMBOL(-3.0,-1.0,0.2,'TRANSVERSE BP FILT',0.0,18)
      CALL SYMBOL(-3.0,-1.6,0.15,'S/N',0.0,3)
      CALL NUMBER(-2.0,-1.6,0.15,TSQD(2),0.0,2)
      CALL PLOT(0.0,0.0,3)
      CALL PLTRTN(FIN(1,2),NTDIM,2.0,TIMEL,TIMER,TIMEE,SF)
      CALL SYMBOL(-3.0,0.3,0.15,'S.F.',0.0,4)
      CALL NUMBER(-2.5,0.3,0.15,SF,0.0,6)
      CALL PLOT(0.0,0.0,3)
```

```
      CALL SYMBOL(-3.0,-1.0,0.2,'RADIAL BP FILT',0.0,14)
      CALL SYMBOL(-3.0,-1.6,0.15,'S/N',0.0,3)
      CALL NUMBER(-2.0,-1.6,0.15,TSQD(3),0.0,2)
      CALL PLOT(0.0,0.0,3)
      CALL PLTRTN(FIN(1,3),NTDIM,2.0,TIMEL,TIMER,TIMEE,SF)
      CALL SYMBOL(-3.0,0.3,0.15,'S.F.',0.0,4)
      CALL NUMBER(-2.5,0.3,0.15,SF,0.0,6)
      CALL PLOT(0.0,0.0,3)
C
C     *****   TERMINATE   *****
C
      ENTDIM=NTDIM
      FINUP=(ENTDIM/50.0)+4.0
      CALL PLOT(FINUP,0.0,-3)
 9998 CALL PLOT (0.0,0.0,998)
      RETURN
      END
```

SUBROUTINE SCALAD

```
      SUBROUTINE SCALAD(DATA,PROC,NTDIM,SCFAC,TILQ)
      DIMENSION DATA(2100,3),PROC(2100,3)
      DIMENSION TEMP(2100,3)
      ISTART=TILQ/2.
      NTDIM=NTDIM/2
      DO 10 J=1,3
      DO 10 I=1,NTDIM
      TEMP(I,J)=0.0
   10 CONTINUE
      DO 20 J=1,3
      DO 20 I=ISTART,NTDIM
      TEMP(I,J)=DATA(I+NTDIM,J)
   20 CONTINUE
      DO 30 J=1,3
      DO 30 I=1,NTDIM
      PROC(I,J)=TEMP(I,J)*SCFAC+DATA(I,J)
   30 CONTINUE
      RETURN
      END
```

SUBROUTINE RMS

```
      SUBROUTINE RMS(PROC,CTIME,TSQD,TIL,TIE,F,TEMP,ISUM)
      DIMENSION F(3)
      DIMENSION PROC(2100,3),TSQD(3),CTIME(3),T(3),TEMP(3)
      DO 1 J=1,3
      F(J)=0.0
      TSQD(J)=0.0
      CTIME(J)=0.0
      TEMP(J)=0.0
      T(J)=0.
      IF(ISUM.NE.0) GO TO 5
      NL=TIL/4.
      GO TO 6
    5 NL=TIL/2.
    6 NL=NL-20
      ANL=NL
      DO 15 I=1,NL
      T(J)=T(J)+PROC(I,J)**2
15    CONTINUE
      IF(T(J).GT.0.0) GO TO 17
      F(J)=0.0
      TSQD(J)=0.0
      CTIME(J)=0.0
      TEMP(J)=0.0
      WRITE(3,16)
   16 FORMAT(5X,'+++++  DATA TRACE HAS BEEN ZEROED  +++++')
      GO TO 1
   17 F(J)=SQRT(T(J)/ANL)
      F(J)=20.*ALOG10(F(J))
      TEMP(J)=0.0
      NE=TIE/2.
      IF(ISUM.NE.0) GO TO 18
      NL=2*NL
   18 DO 20 I=NL,NE
      IF(ABS(PROC(I,J)).GT.ABS(TEMP(J))) GO TO 10
      GO TO 20
   10 ID=I
      TEMP(J)=PROC(I,J)
   20 CONTINUE
      CTIME(J)=2*ID
      TSQD(J)=ABS(TEMP(J))
      TSQD(J)=20.*ALOG10(TSQD(J))-F(J)
1     CONTINUE
      RETURN
      END
```

SUBROUTINE LOVFIL

```
      SUBROUTINE LOVFIL(PBUF,IPTSEG,ANGBET)
      DIMENSION PBUF(64,3,2)
      RRSHI=0.0
      TRSHI=0.0
      PHI=0.0
      TISHI=0.0
      BETA=0.0
      TRROT=0.0
      TIROT=0.0
      TRUNSH=0.0
      TIUNSH=0.0
      PTSEG=IPTSEG
      CONVRD=180.0/3.14159
      DO 60 I=3,IPTSEG,2
      IF(PBUF(I+1,1,1))10,20,10
   10 PHI=ATAN2(PBUF(I+1,1,1),PBUF(I,1,1))
      GO TO 30
   20 PHI=0.0
C
C          SHIFT TIME ORIGIN
C
   30 RRSHI=PBUF(I,3,1)*COS(PHI)+PBUF(I+1,3,1)*SIN(PHI)
      TRSHI=PBUF(I,2,1)*COS(PHI)+PBUF(I+1,2,1)*SIN(PHI)
      TISHI=PBUF(I+1,2,1)*COS(PHI)-PBUF(I,2,1)*SIN(PHI)
      RISHI=PBUF(I+1,3,1)*COS(PHI)-PBUF(I,3,1)*SIN(PHI)
C
C          COMPUTE AND TEST BETA
C
      BARG=RRSHI/TRSHI
      BETA=ATAN(BARG)
      DEGBET=BETA*CONVRD
      ABSBET=ABS(DEGBET)
      IF(ABSBET.GT.ANGBET) GO TO 40
C
C          ROTATE BY MINUS BETA
C
      TRROT=TRSHI*COS(BETA)-RRSHI*SIN(BETA)
      TIROT=TISHI*COS(BETA)-RISHI*SIN(BETA)
C
C          SHIFT BACK TO ORIGINAL TIME ORIGIN
C
      TRUNSH=TRROT*COS(PHI)-TIROT*SIN(PHI)
      TIUNSH=TRROT*SIN(PHI)+TIROT*COS(PHI)
      GO TO 50
   40 TRUNSH=0.0
      TIUNSH=0.0
   50 PBUF(I,2,1)=TRUNSH
      PBUF(I+1,2,1)=TIUNSH
   60 CONTINUE
      RETURN
      END
```

SUBROUTINE RAYFIL

```
      SUBROUTINE RAYFIL(PBUF,IPTSEG,IPOWER)
      DIMENSION PBUF(64,3,2)
      RVPOW=0.0
      RRPOW=0.0
      RVTOT=0.0
      RRTOT=0.0
      DO 50 I=1,IPTSEG,2
      CPRR=PBUF(I,1,1)*PBUF(I,3,1)+PBUF(I+1,1,1)*PBUF(I+1,3,1)
      CPRI=PBUF(I,1,1)*PBUF(I+1,3,1)-PBUF(I+1,1,1)*PBUF(I,3,1)
      IF(CPRI.NE.0.0) GO TO 20
      RFIL=0.0
      GO TO 30
   20 RFIL=CPRI/SQRT(CPRI**2+CPRR**2)
   30 DO 40 J=1,IPOWER
      IF(RFIL.LT..0001) RFIL=0.0
   40 RFIL=RFIL**2
      PBUF(I,1,1)=PBUF(I,1,1)*RFIL
      PBUF(I+1,1,1)=PBUF(I+1,1,1)*RFIL
      PBUF(I,3,1)=PBUF(I,3,1)*RFIL
      PBUF(I+1,3,1)=PBUF(I+1,3,1)*RFIL
   50 CONTINUE
      RETURN
      END
```

SUBROUTINE FILTBP

```
      SUBROUTINE FILTBP(FIN,NTDIM,FLO,FHI,TAPR)
      DIMENSION FIN(2100,3),FILT(2100)
      ENTDIM=NTDIM
      DELTF=1.0/(2.0*ENTDIM)
      FST=((FLO-TAPR)/DELTF)*2.0
      FLOO=(FLO/DELTF)*2.0
      FHII=(FHI/DELTF)*2.0
      KST=FST
      KLOO=FLOO
      KHII=FHII
      TANALF=1.0/(FLOO-FST)
      JPTS=KLOO-KST
      KLEN=FHII-KLOO
      DO 100 I=1,NTDIM
      FILT(I)=0.0
  100 CONTINUE
      DO 110 I=1,JPTS
      AI=I
      FILT(I+KST)=AI*TANALF
  110 CONTINUE
      DO 120 I=1,KLEN
      FILT(KLOO+I)=1.0
  120 CONTINUE
      AJPTS=JPTS
      DO 130 I=1,JPTS
      AI=I
      FILT(KHII+I)=(AJPTS-AI)*TANALF
  130 CONTINUE
      DO 200 J=1,3
      DO 200 I=1,NTDIM
      FIN(I,J)=FIN(I,J)*FILT(I)
  200 CONTINUE
      RETURN
      END
```

SUBROUTINE PLTRTN

```
      SUBROUTINE PLTRTN(DATA,NPTS,T,TL,TR,TE,SF)
      DIMENSION DATA(NPTS)
      EN=NPTS
      ALENGT=(EN*T)/100.0
      TIL=(-ALENGT+TL*.01)
      TIR=(-ALENGT+TR*.01)
      TIE=(-ALENGT+TE*.01)
      KALENG=ALENGT
      DIST=KALENG
      FINLEN=ALENGT-DIST
      BLENGT=-ALENGT
      DX=-0.01*T
      S=0.0
      DO 5 I=1,NPTS
    5 IF(ABS(DATA(I)).GT.S) S=ABS(DATA(I))
      IF(S.EQ.0.0) GO TO 7
      SF=0.6/S
      GO TO 8
    7 SF=0.0
    8 CALL PLOT(0.0,-0.8,-2)
      DO 1 KK=1,KALENG
      CALL PLOT (1.0,0.0,2)
      CALL PLOT (1.0,0.1,2)
      CALL PLOT (1.0,-0.1,2)
    1 CALL PLOT (1.0,0.0,-2)
      CALL PLOT (FINLEN,0.0,-1)
      CALL PLOT(TIE,0.0,3)
      CALL PLOT(TIE,-0.6,2)
      CALL PLOT(TIR,0.0,3)
      CALL PLOT(TIR,-0.6,2)
      CALL PLOT(TIL,0.0,3)
      CALL PLOT(TIL,-0.6,2)
      CALL PLOT(TIL,0.0,2)
      EX=0.0
      EYE=DATA(NPTS)*SF
      CALL PLOT(DX,EYE,3)
      DO 2 J=1,NPTS
      EX=EX+DX
      JJ=NPTS-J+1
      EY=DATA(JJ)*SF
    2 CALL PLOT (EX,EY,2)
      CALL PLOT (BLENGT,0.0,3)
      CALL PLOT (BLENGT,-0.8,-2)
      RETURN
      END
```

APPENDIX B
DETECTION STATISTICS

The figures of this appendix give the detection statistics for southern Kamchatka (SKAM) single-site data, central Asia (CENA) single-site data, and central Asia (CENA) beam data. The upper portion of each figure shows a histogram indicating the number of detected and non-detected events for each m_b increment. The lower portion of each figure shows the maximum likelihood detectability curve for the statistics represented by the histogram.

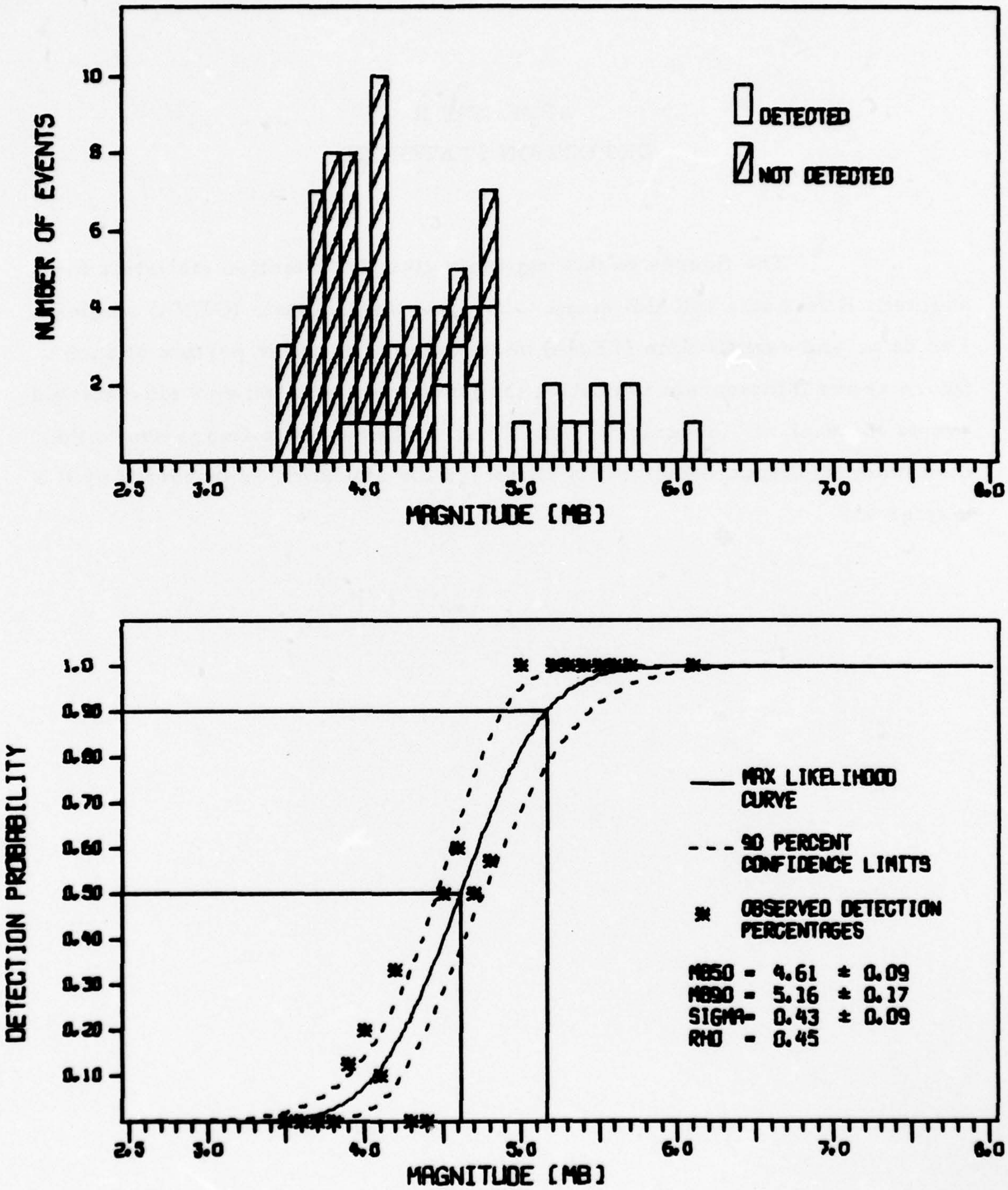

FIGURE B-1

DETECTION STATISTICS FOR SKAM BANDPASS FILTERED LR-V COMPONENT - SINGLE-SITE DATA

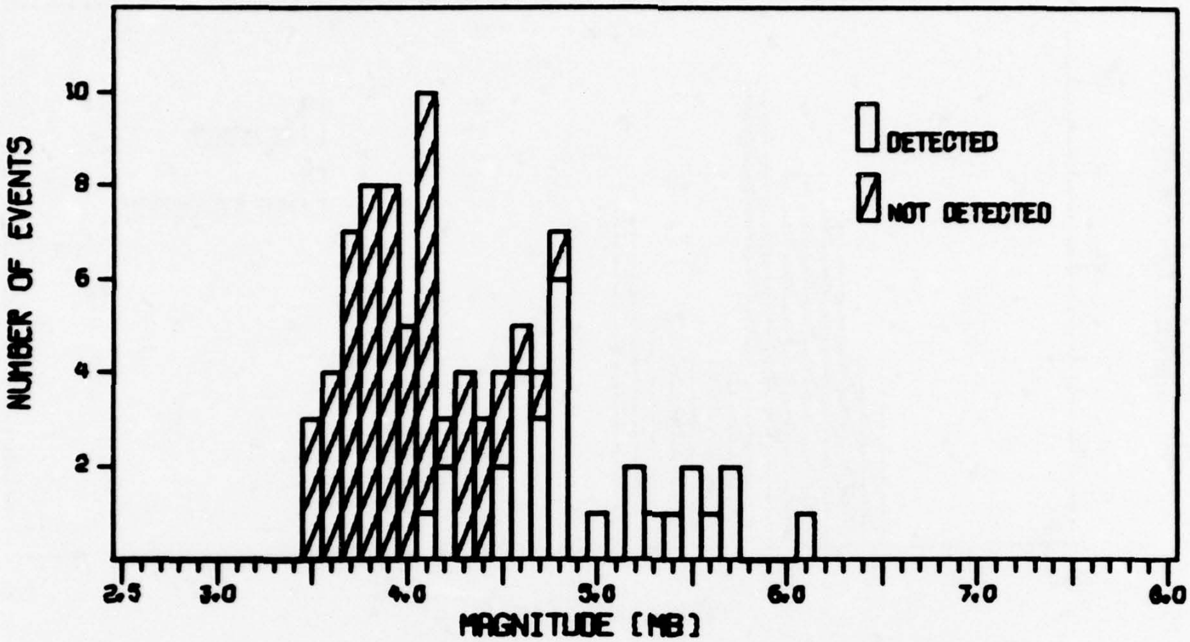

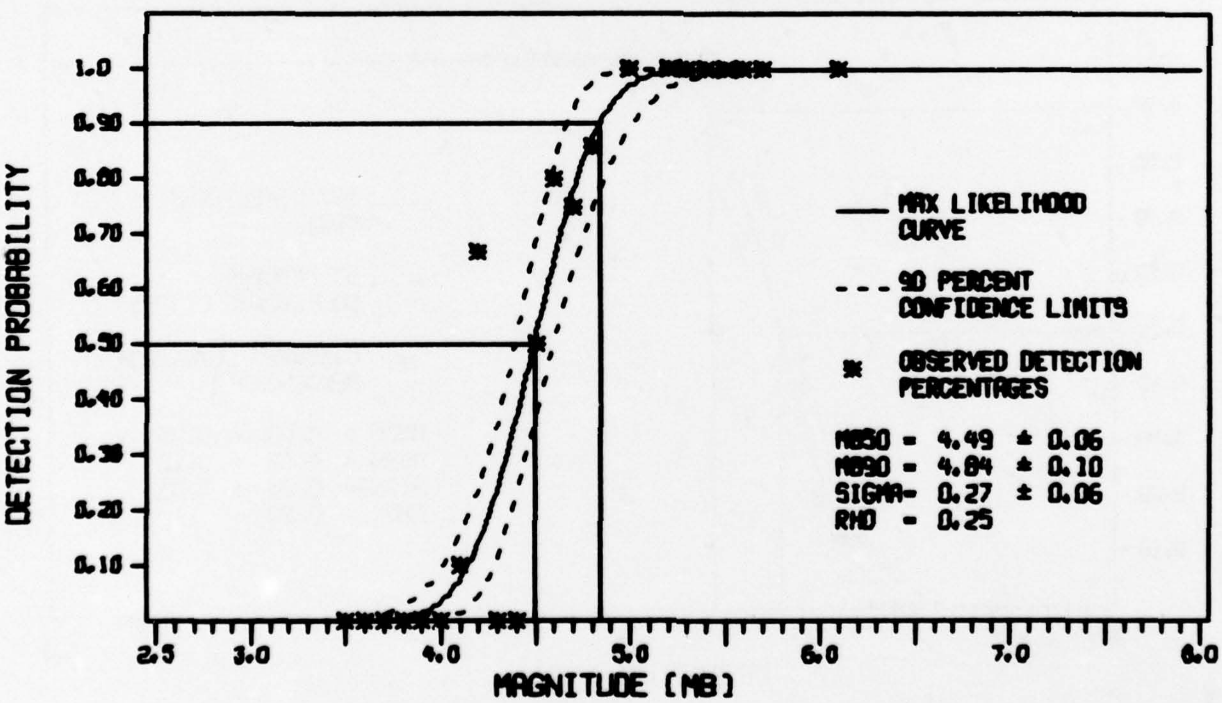

FIGURE B-2

DETECTION STATISTICS FOR SKAM BANDPASS FILTERED
LQ-T COMPONENT - SINGLE-SITE DATA

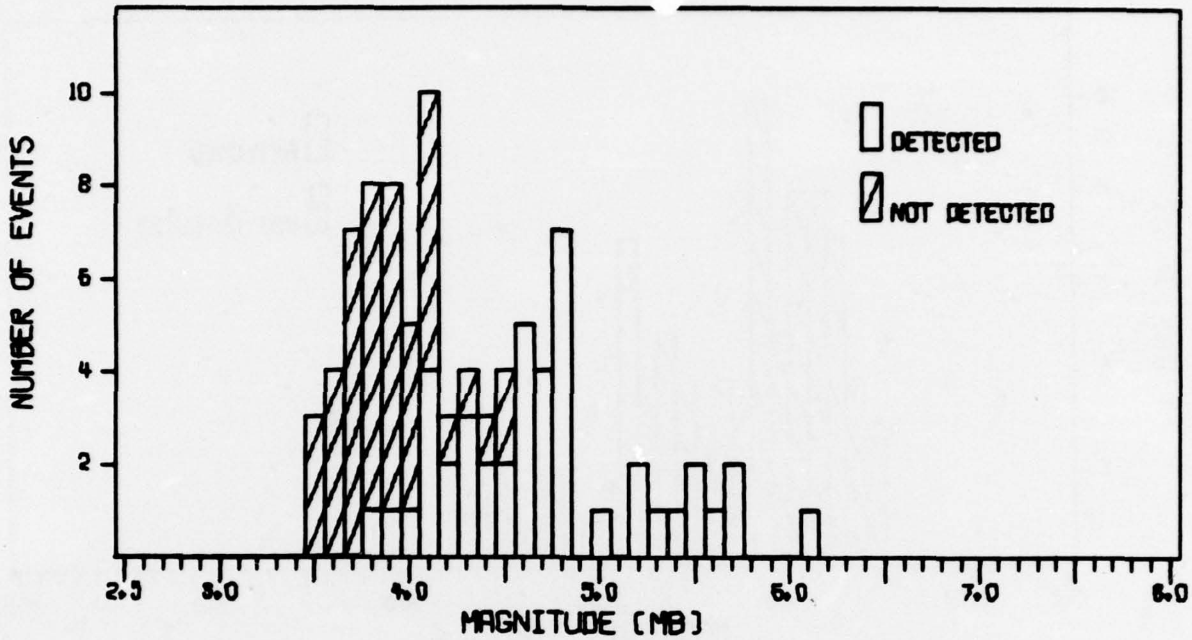

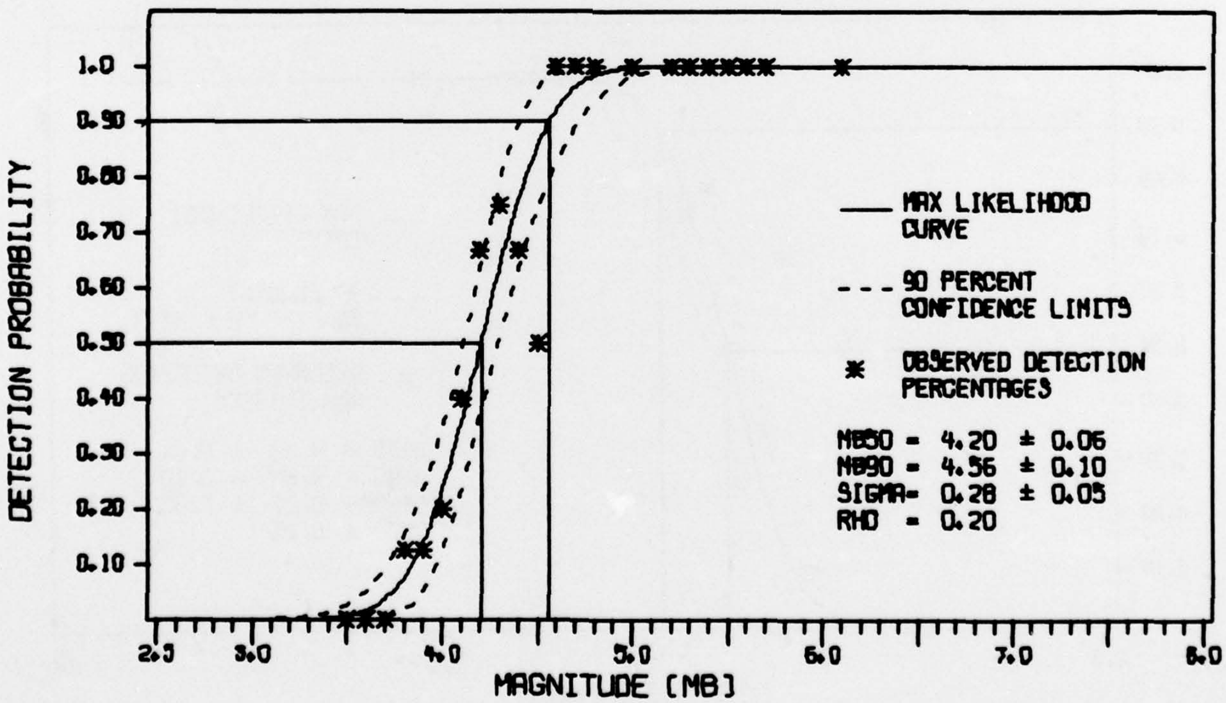

FIGURE B-3

DETECTION STATISTICS FOR SKAM ORIGINAL TCA PROCESSED LR-V COMPONENT - SINGLE-SITE DATA

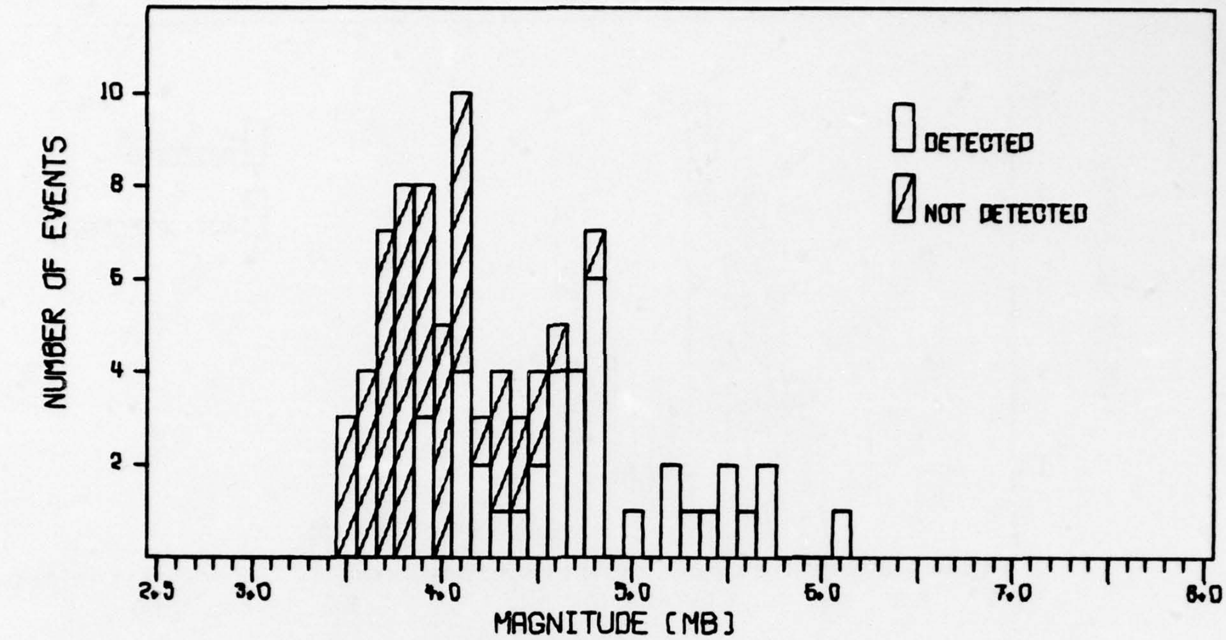

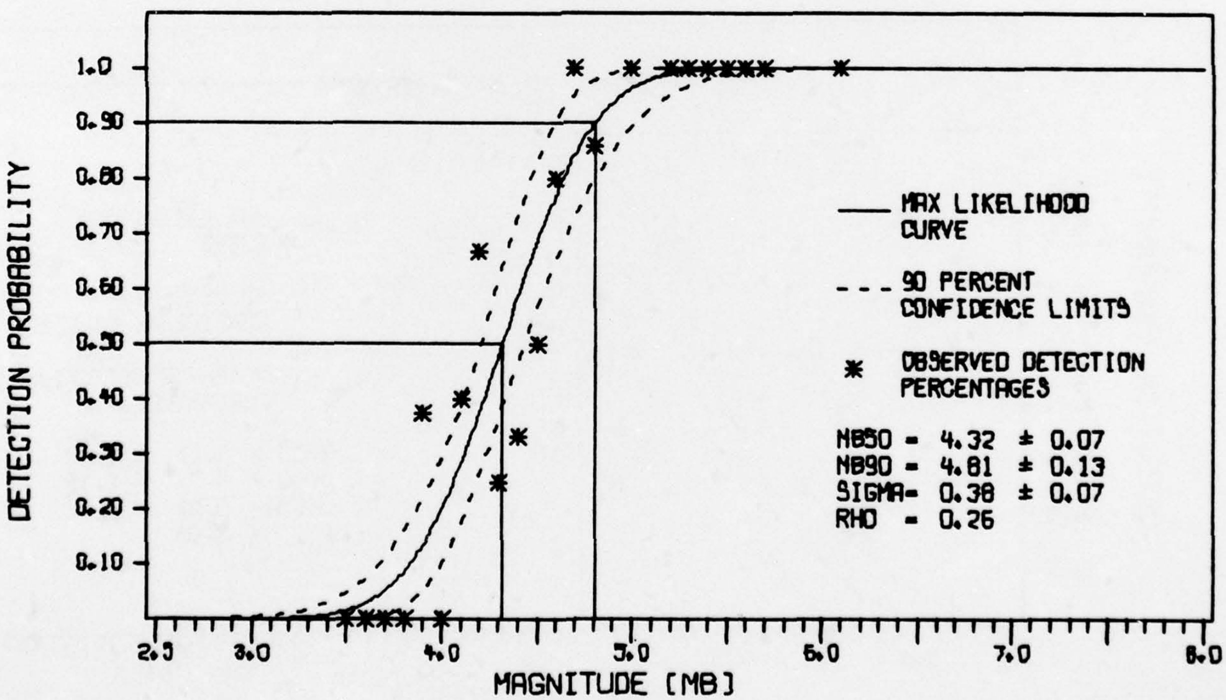

FIGURE B-4

DETECTION STATISTICS FOR SKAM ORIGINAL TCA PROCESSED LQ-T COMPONENT - SINGLE-SITE DATA

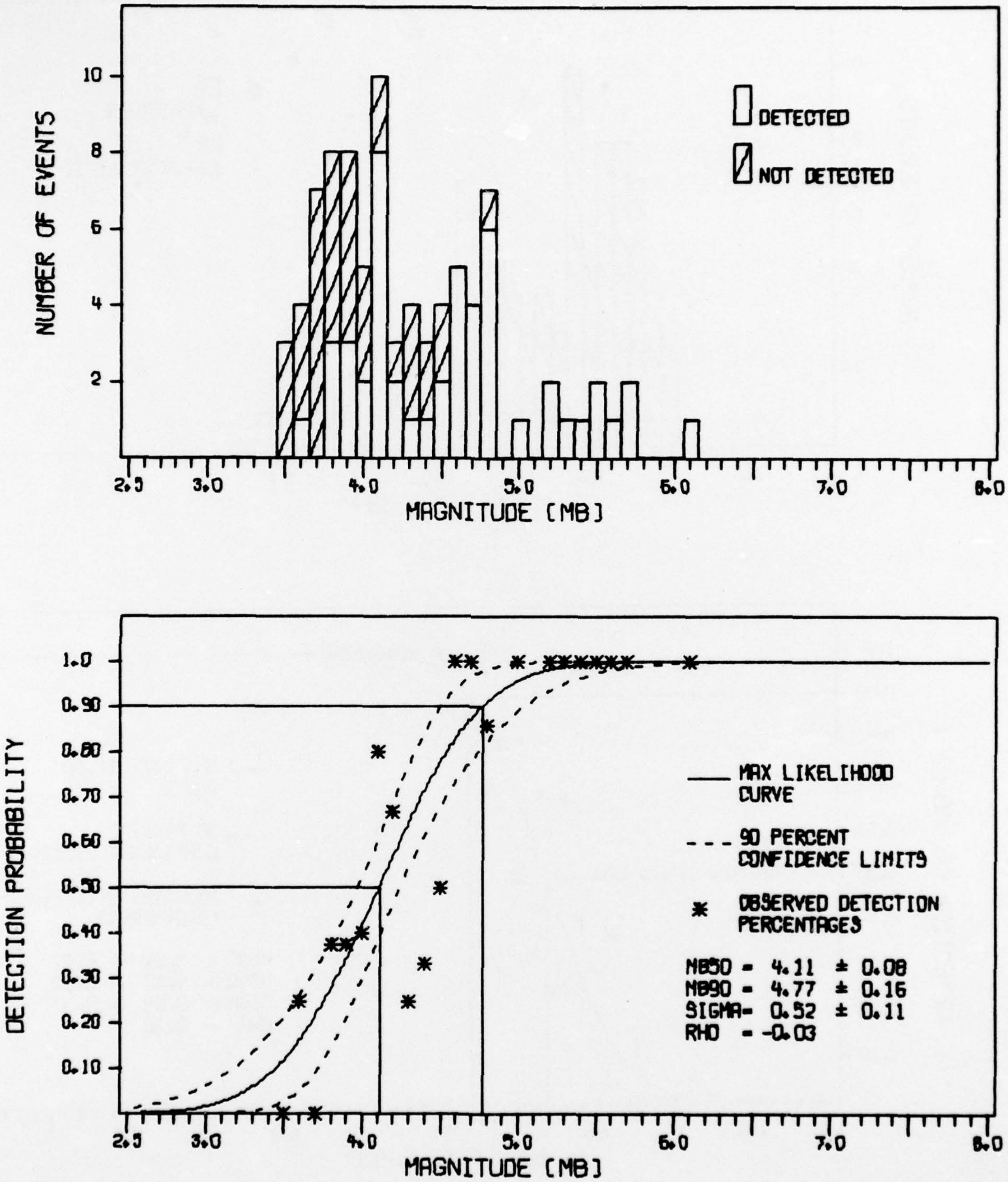

FIGURE B-5

DETECTION STATISTICS FOR SKAM NEW TCA PROCESSED LQ-T COMPONENT - SINGLE-SITE DATA

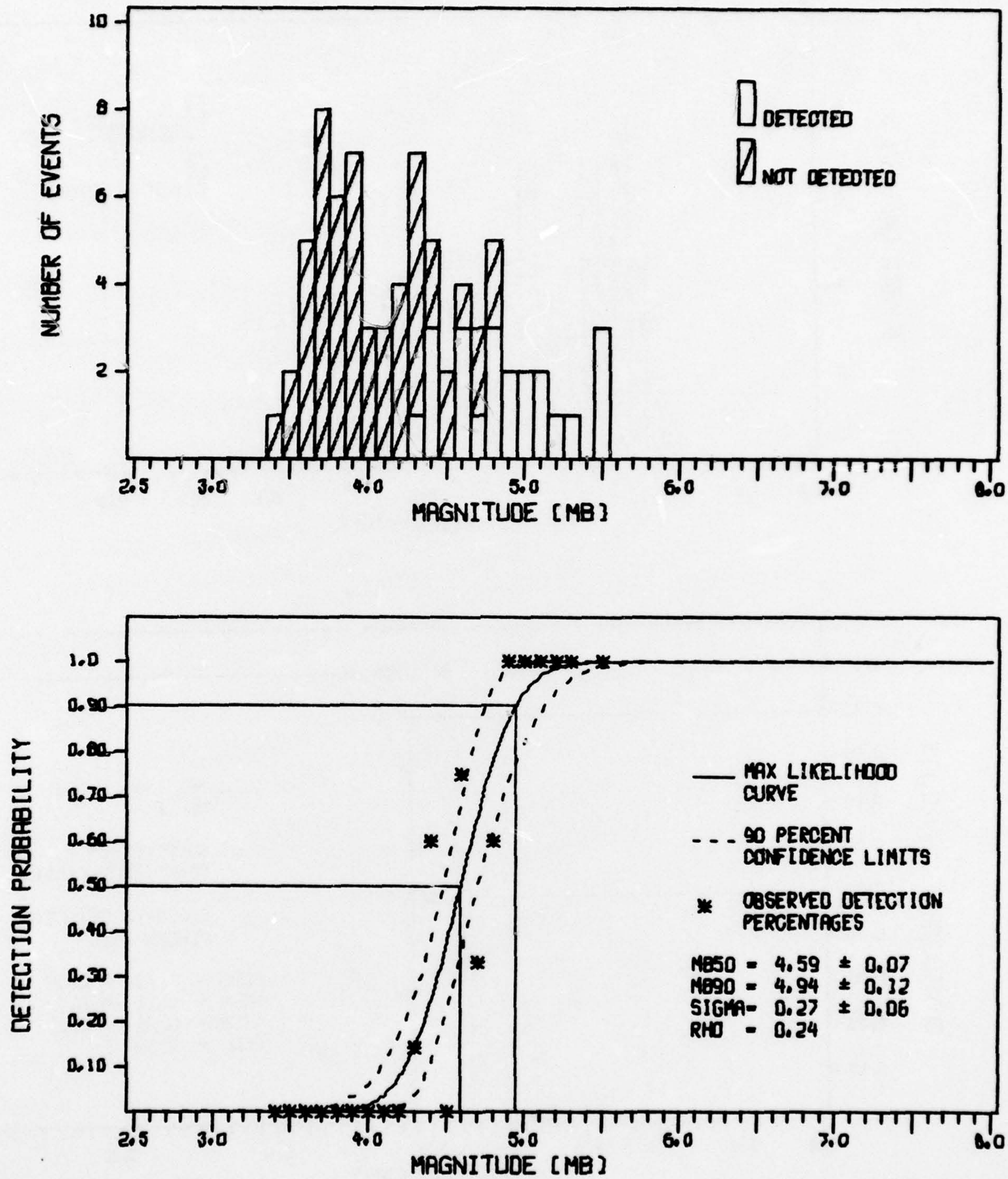

FIGURE B-6

DETECTION STATISTICS FOR CENA BANDPASS FILTERED
LR-V COMPONENT - SINGLE-SITE DATA

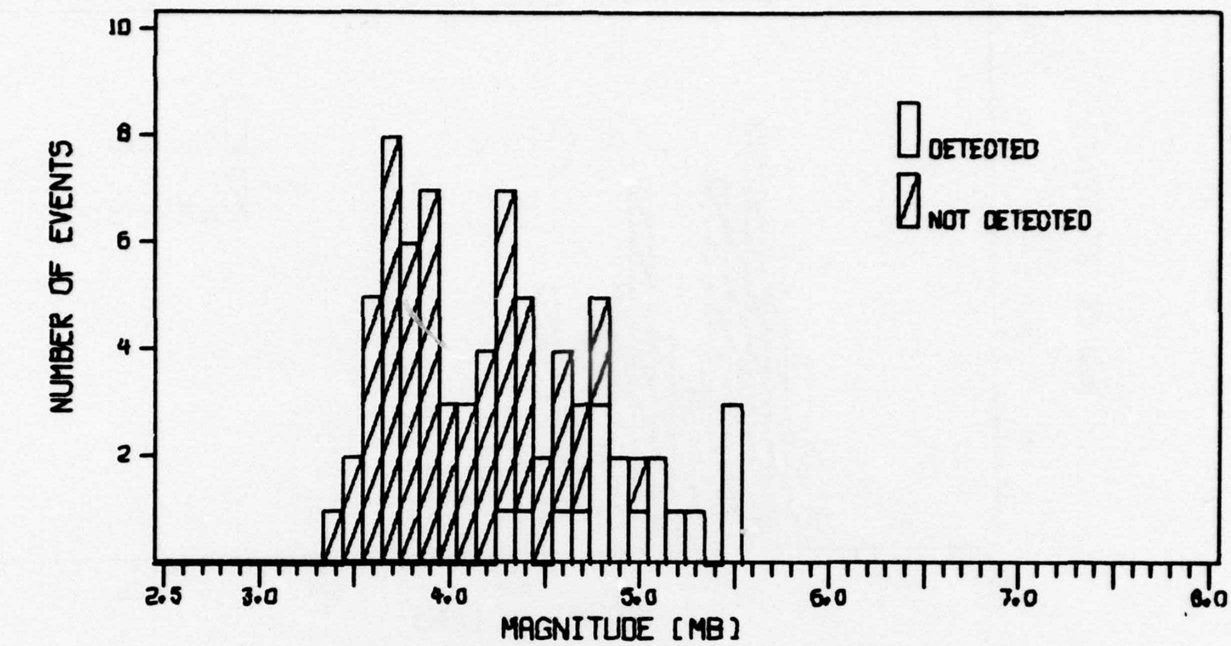

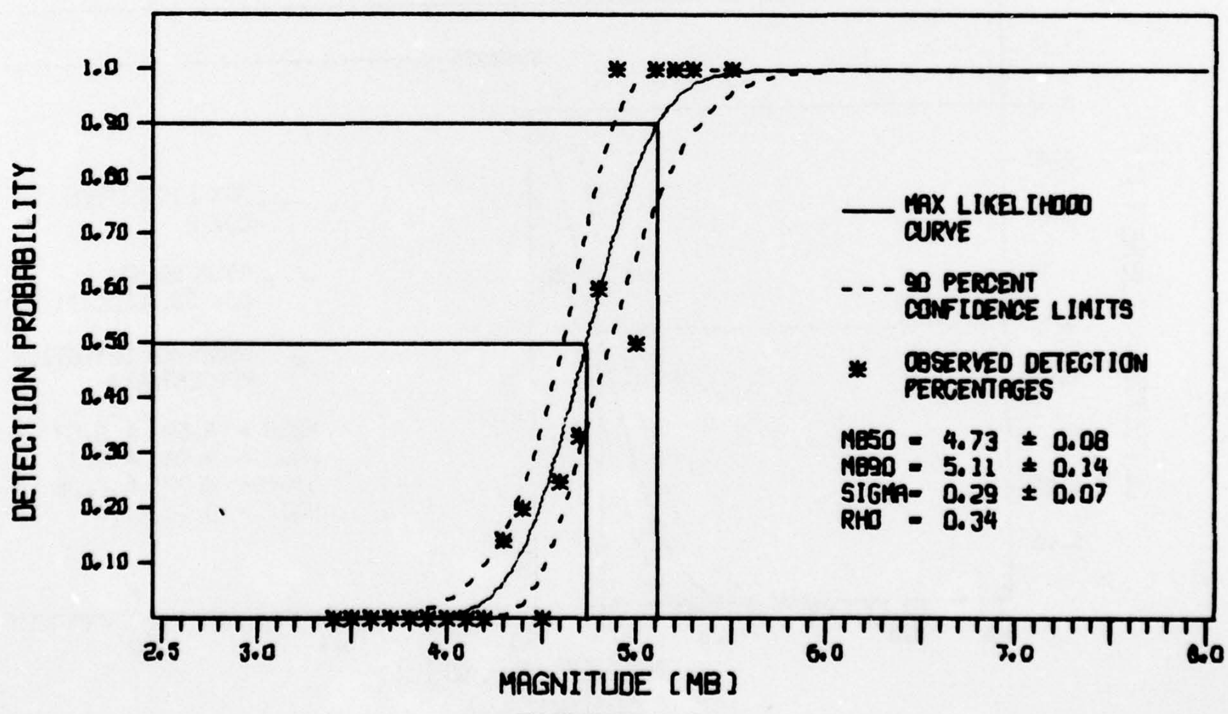

FIGURE B-7

DETECTION STATISTICS FOR CENA BANDPASS FILTERED
LQ-T COMPONENT - SINGLE-SITE DATA

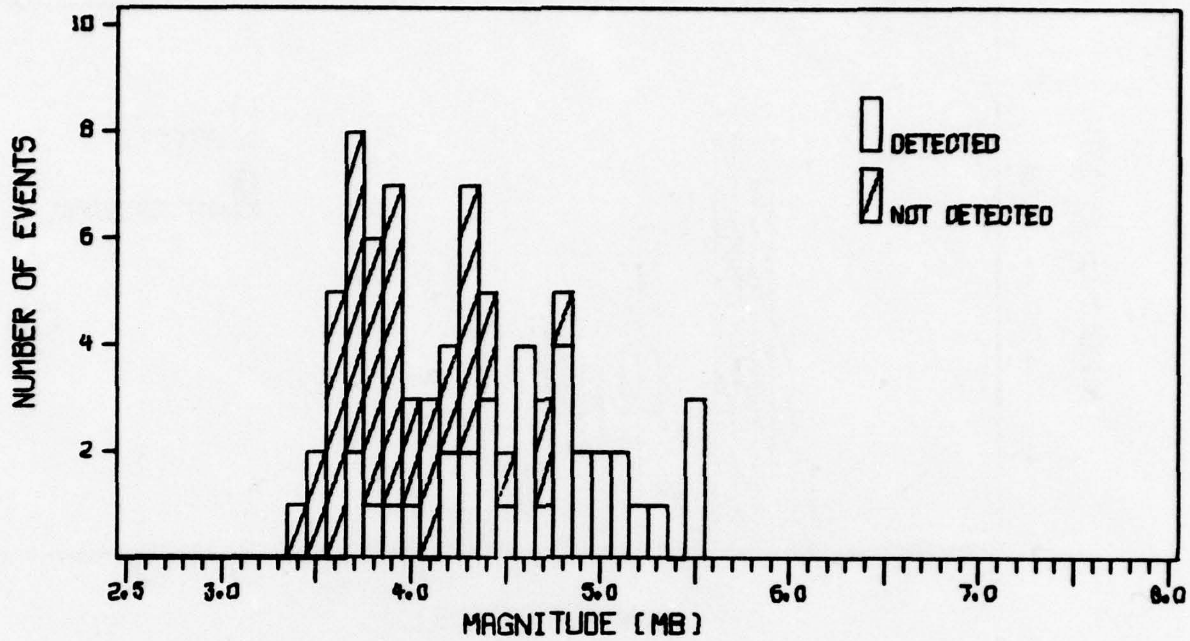

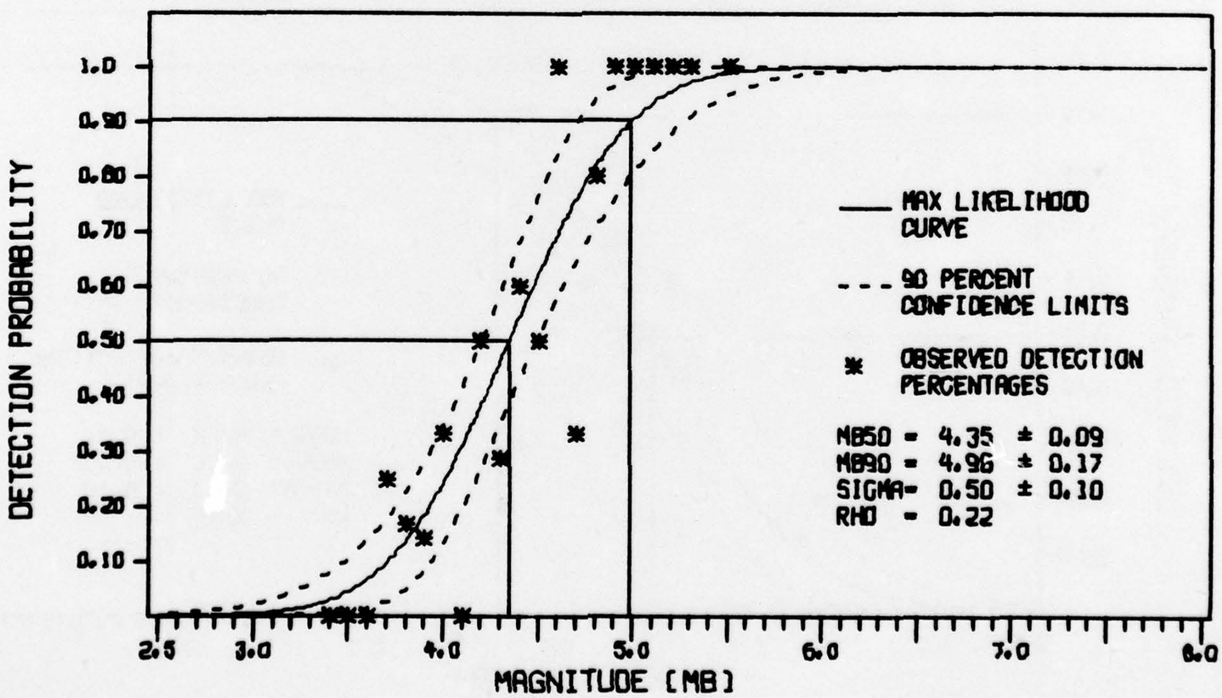

FIGURE B-8

DETECTION STATISTICS FOR CENA ORIGINAL TCA PROCESSED LR-V COMPONENT - SINGLE-SITE DATA

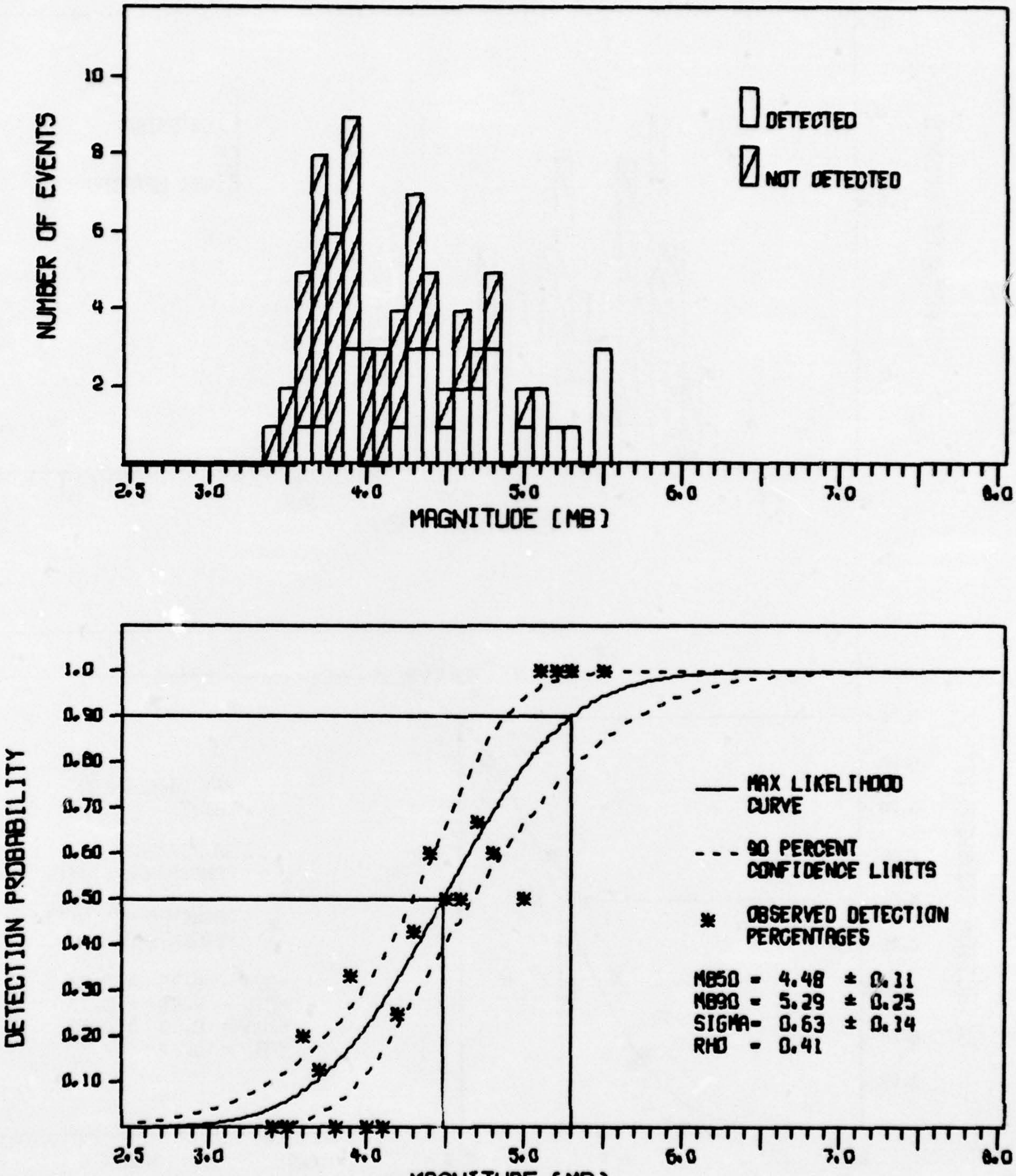

FIGURE B-9

DETECTION STATISTICS FOR CENA ORIGINAL TCA PROCESSED LQ-T COMPONENT - SINGLE-SITE DATA

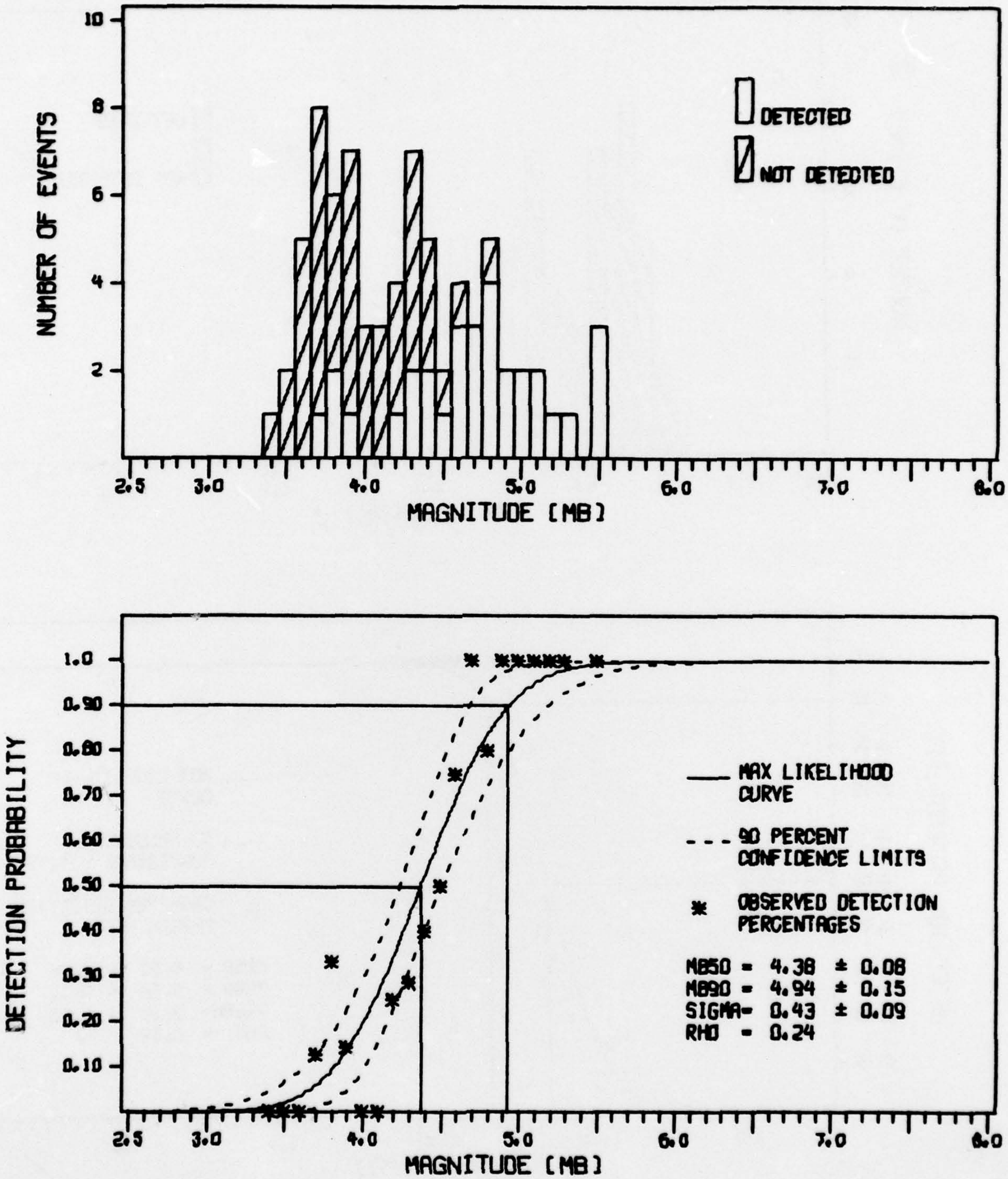

FIGURE B-10

DETECTION STATISTICS FOR CENA NEW TCA PROCESSED
LQ-T COMPONENT - SINGLE-SITE DATA

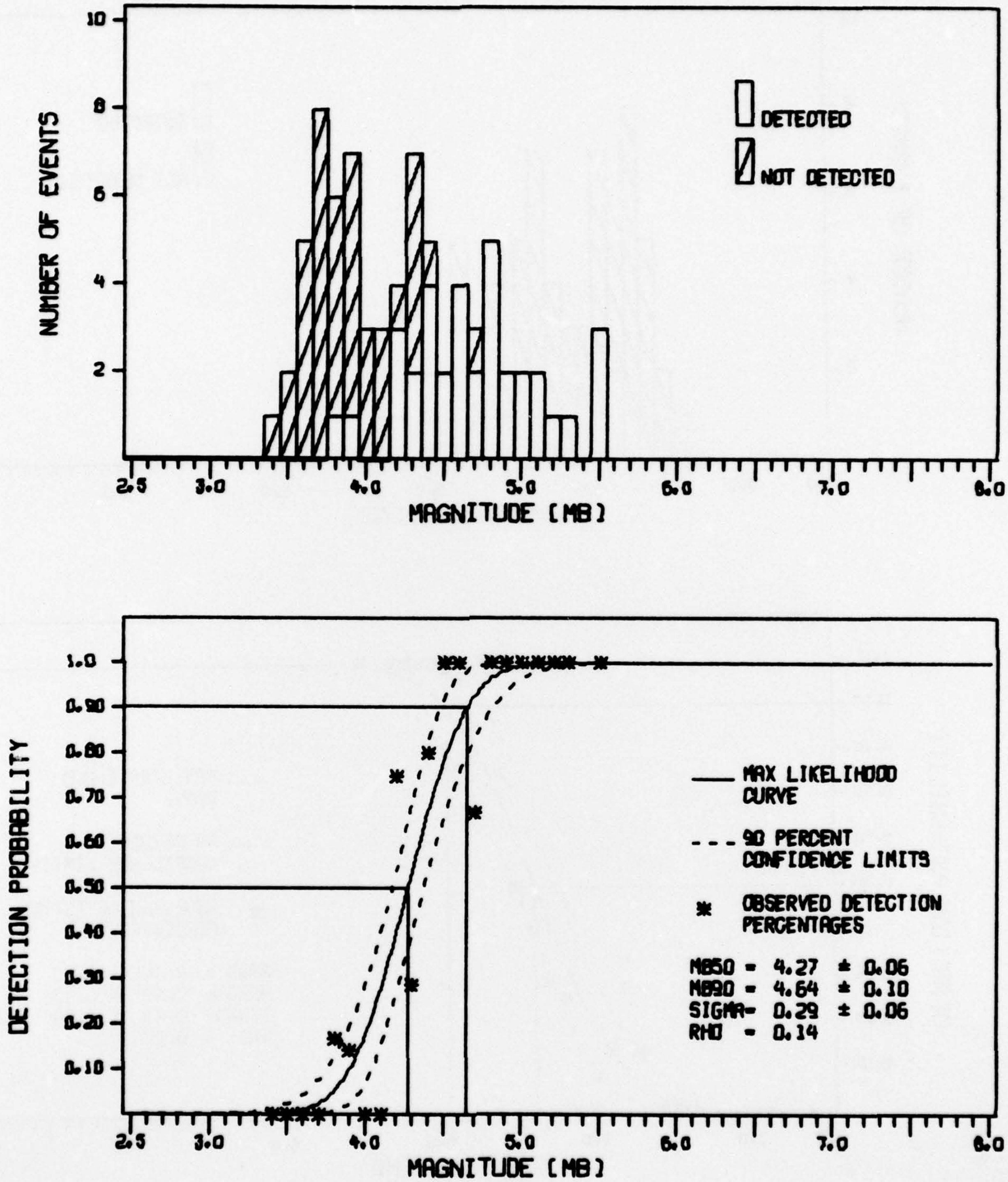

FIGURE B-11

DETECTION STATISTICS FOR CENA BANDPASS FILTERED LR-V COMPONENT - BEAM DATA

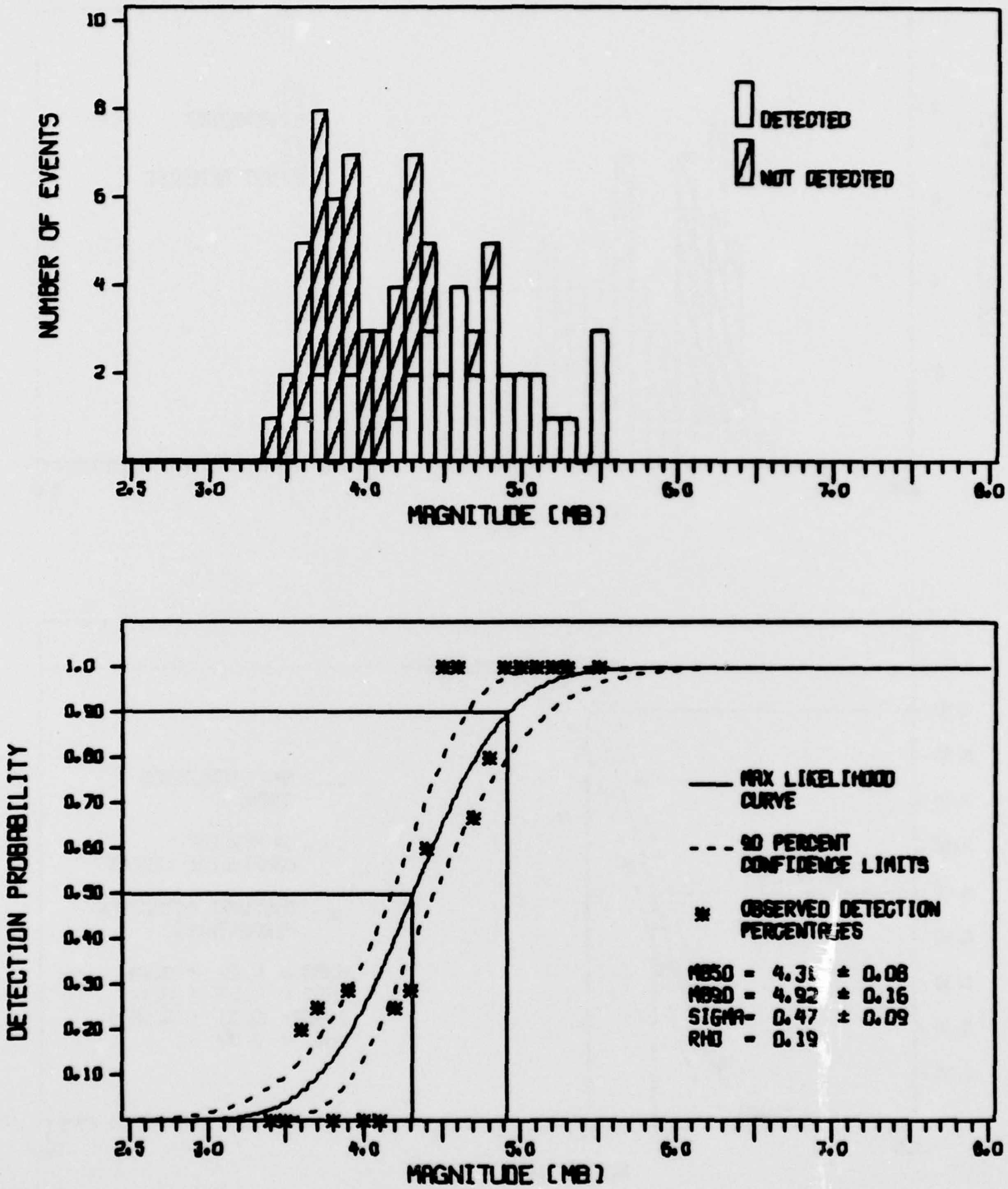

FIGURE B-12

DETECTION STATISTICS FOR CENA BANDPASS FILTERED LQ-T COMPONENT - BEAM DATA

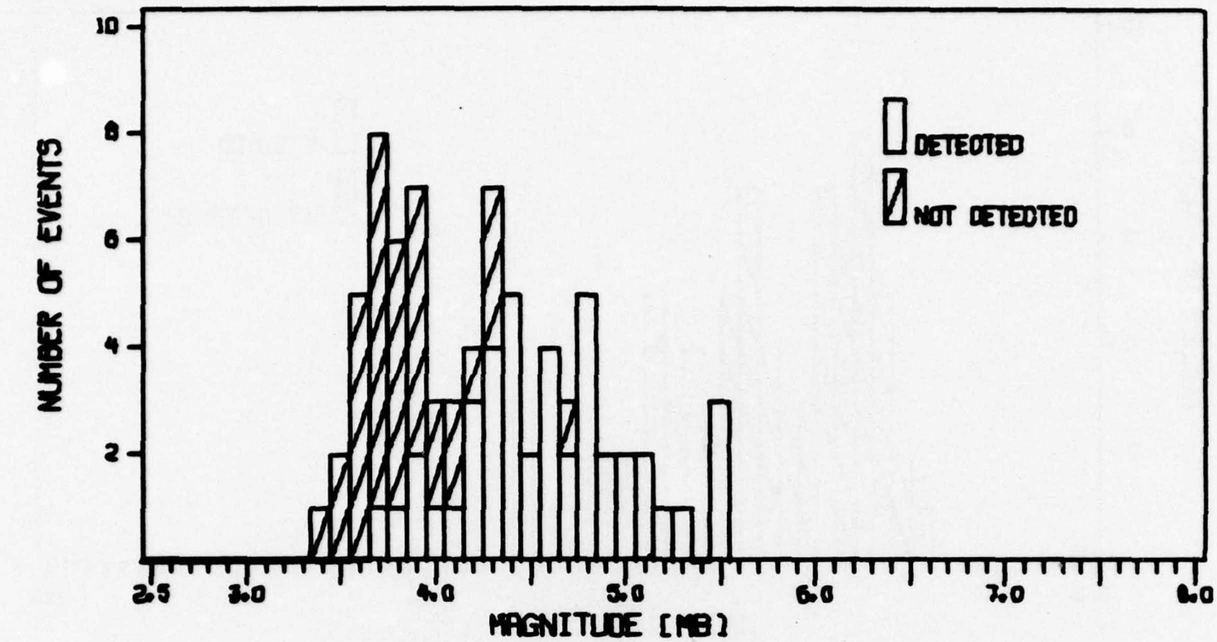

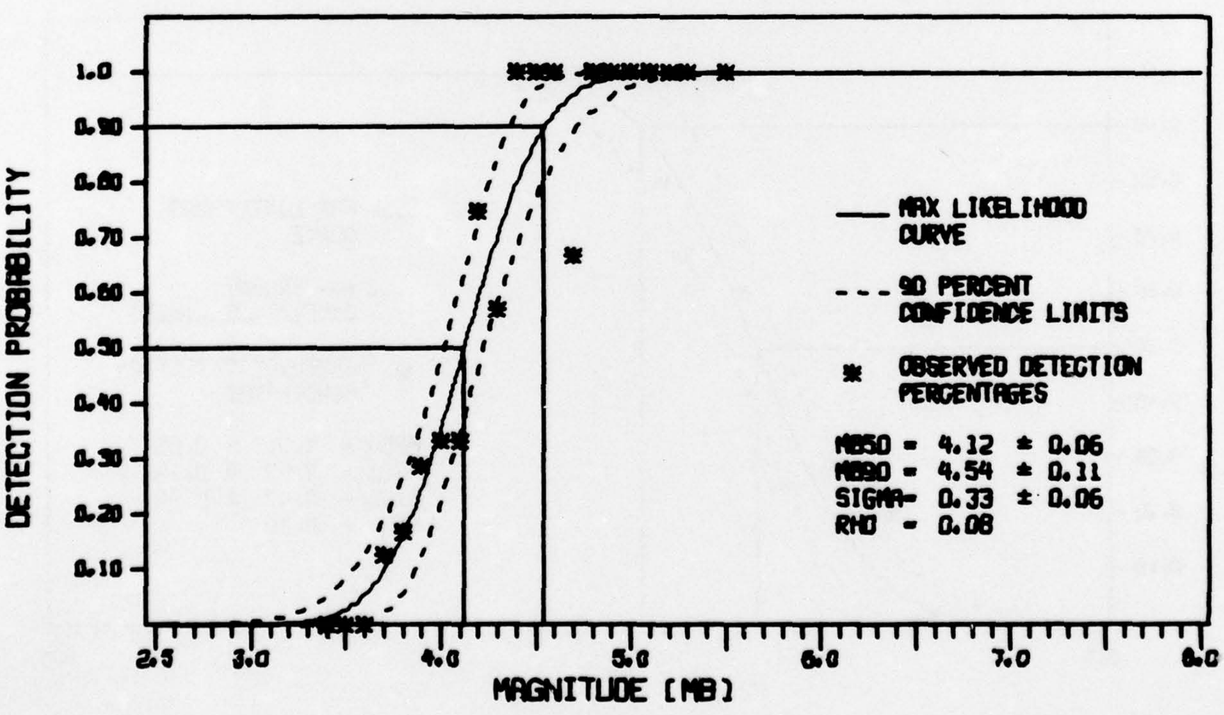

FIGURE B-13

DETECTION STATISTICS FOR CENA ORIGINAL TCA PROCESSED
LR-V COMPONENT - BEAM DATA

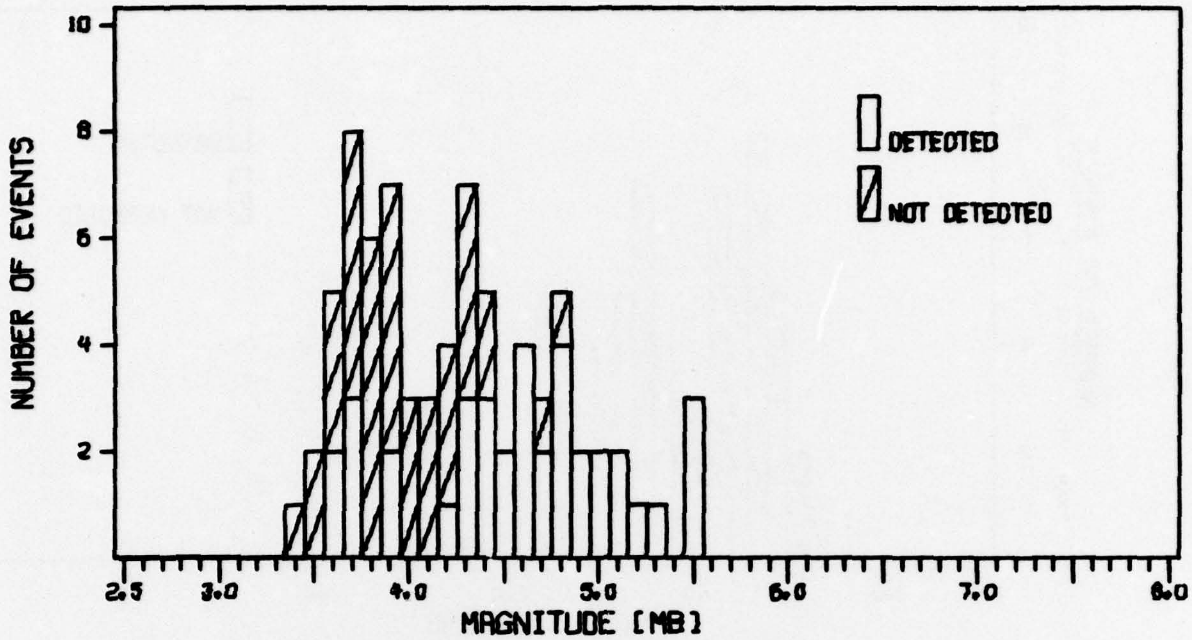

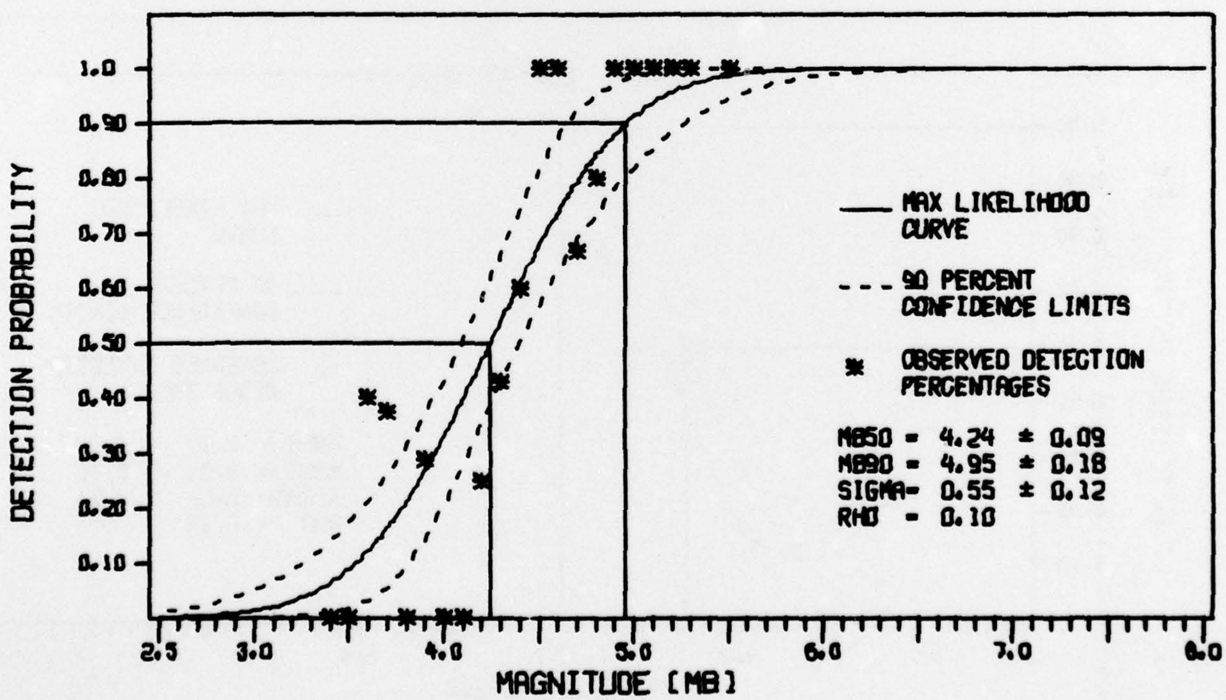

FIGURE B-14

DETECTION STATISTICS FOR CENA ORIGINAL TCA PROCESSED LQ-T COMPONENT - BEAM DATA

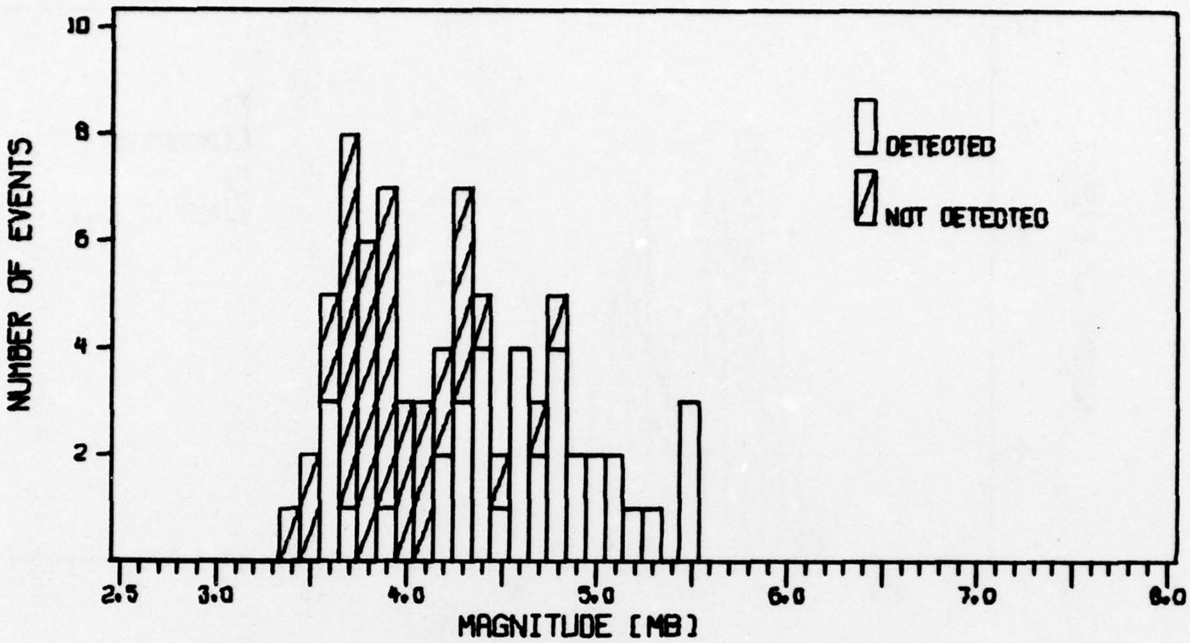

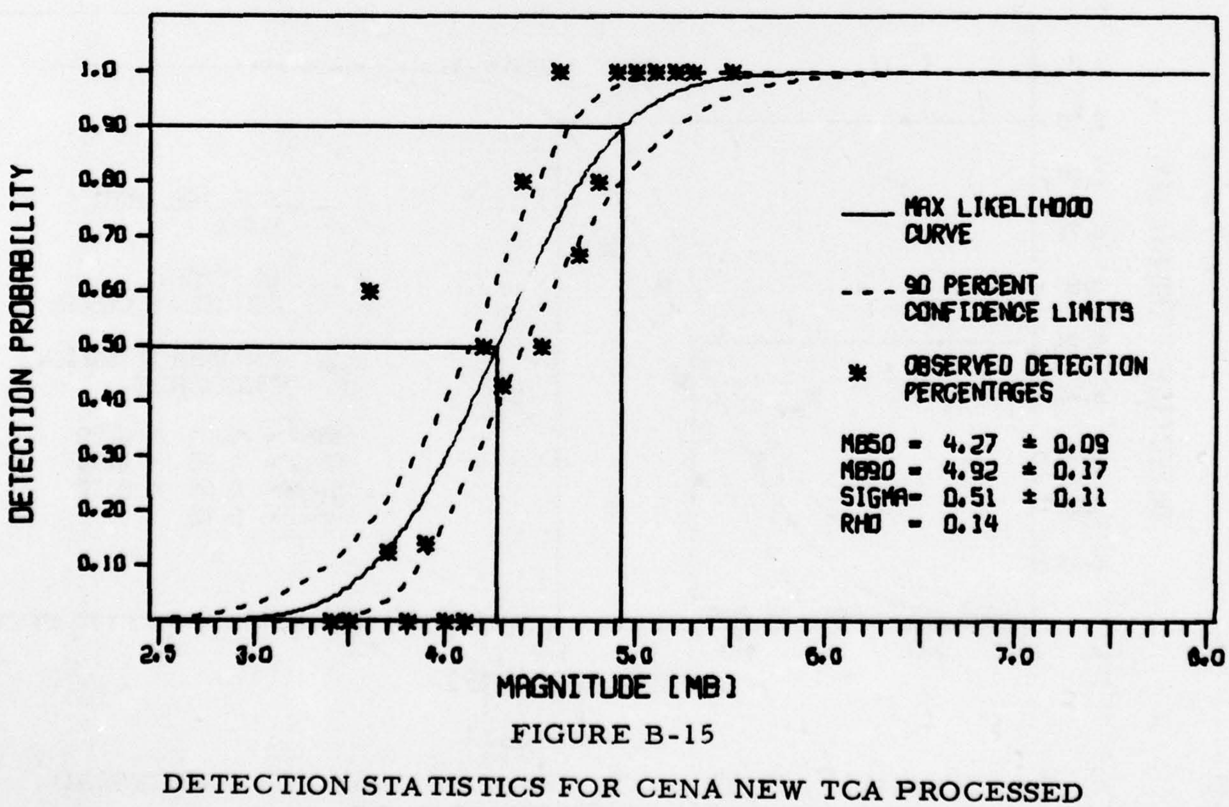

FIGURE B-15

DETECTION STATISTICS FOR CENA NEW TCA PROCESSED
LQ-T COMPONENT - BEAM DATA